Evaluation of radio-resistance mechanisms in cancer stem-like cells isolated from canine tumor cell lines and stem cell-selective radio-sensitizing property of anti-diabetic agent metformin

犬腫瘍細胞株におけるがん幹細胞の放射線耐性機序および
抗糖尿病薬メトホルミンの幹細胞選択的放射線増感効果に関する基礎的研究

Tatsuya　Deguchi

ABSTRACT

Radiation therapy for tumors has become more important treatment modality for human and animal cancer patients. However, tumors re-growth after radiation therapy and ultimately lead to death without cure, even a good response at first. Tumor recurrence after radiation therapy is thought to be due to radio-resistant cells in the tumor cells, and radio-resistant cells surviving after radiation can cause tumor recurrence. Therefore, identifying and characterizing these radio-resistant cells is necessary for establishment novel therapeutic strategy. The aim of this study is to elucidate the existence of Cancer stem-like cells (CSCs) as a cause of the resistance to radiation therapy of dog tumor, and to analyze their characteristic, which can contribute to establish novel strategy for targeting CSCs and improving patient outcome. CSCs derived from canine tumor cell lines were investigated to determine whether they possess the same characteristics of human CSCs, and whether they show lower radiosensitivity than their corresponding parent cells. Then, to search drugs effective for CSCs and elucidate the mechanism of radiation resistance of CSCs, the effect and mechanism of metformin as a radio-sensitizer were evaluated in CSCs.

In chapter I, to isolate CSCs from canine cancer cell lines and to elucidate relation between canine CSCs and radio-sensitivity of tumor, spheroid cells (SCs) were isolated from four canine tumor cell lines (osteosarcoma, melanoma, traditional cell carcinoma, and lung adenocarcinoma) by the culture using sphere formation and evaluated if they have CSCs-like properties, including expression of CSCs makers, tumorigenic capacity, and radio-sensitivity. All SCs isolated using sphere formation

showed high *CD133* expression and tumorigenic ability compared to parental adherent cells (ACs) in normal culture condition. All SCs were significantly resistant against X-irradiation compared to ACs. In addition, the amount of DNA double strand breaks after X-irradiation was significantly lower in SC than in the corresponding AC. These results showed that SCs isolated via sphere formation possess CSCs-like characteristics and CSCs are important factor that affect radiosensitivity in canine tumors.

In chapter II, to establish therapeutic strategy targeting CSCs, the radio-sensitizing effect of metformin and its mechanism of anti-cancer effect were investigated. It has been reported metformin has many anti-cancer effect, alone or in the combination with ionizing radiation. However, the mechanism underlying its radio-sensitized effect is still unclear, especially for CSCs. SCs was isolated from a canine osteosarcoma cell line by sphere formation culture of original ACs, and used as radio-resistance CSCs model. The radio-sensitizing effect of metformin was examined by using clonogenic assay, and it was revealed the mechanism of its radio-sensitization focusing on mitochondrial function. Metformin preferentially radio-sensitized SCs leading to inhibiting mitochondrial respiration, as determined by the induction of intracellular ROS, decrease of oxygen consumption, ATP, and mitochondrial membrane potential. Additionally, to elucidate high sensitivity of radio-sensitizing effect of metformin to SCs as compared with ACs, the respiratory ability of mitochondria was evaluated and SCs had a higher ability of mitochondrial respiration than ACs. According to these results, mitochondrial respiration might play a central role in the radio-resistance mechanism of CSCs and metformin is a promising radio-sensitizer that can inhibit mitochondrial respiration of CSCs.

In conclusion, CSCs were shown to be important as a factor determining

radiosensitivity in canine tumors. In addition, metformin targeting mitochondria of radio-resistant CSCs was shown to be effective as a radio-sensitizer, and the possibility that high ability of mitochondrial respiration may be involved in radio-resistance of CSCs has been shown.

ABBREVIATIONS

ACs	adherent cells
ADP	adenosine monophosphate
AMPK	5’ adenosine monophosphate-activated protein kinases
ATP	adenosine triphosphate
bFGF	basic fibroblast growth factor
CCCP	carbonyl cyanide m-chlorophenyl hydrazine
CSCs	cancer stem-like cells
DAPI	4’, 6’-diamidino-2-phenylindole
DMEM	Dulbecco’s modified Eagle’s medium
DSB	double strand break
EGF	epidermal growth factor
ESR	electron spin resonance
ETC	electron transport chain
HE	hematoxylin and eosin
OCR	oxygen consumption ratio
PI3K	phosphoinositide 3-kinase
pO_2	pressure of oxygen
MDR	multi drug resistance proteins
MFI	mean fluorescence intensity
mTOR	mammalian target of rapamycin
MTT	3-[4, 5-dimethylthiazol-2-yl]-2, 5 diphenyl tetrazolium bromide

NHEJ	non-homologous end joining
PE	plating efficiency
RT-PCR	reverse transcription-polymerase chain reactions
ROS	reactive oxygen species
RPMI	Roswell Park Memorial Institute medium
RT	room temperature
SCs	spheroid cells
SD	standard deviation
SF	survival fraction
53BP1	p53-binding protein 1

CONTENTS

PREFACE

Radiation therapy is an effective treatment modality for human and animal cancer patients. In the last decades, the advent of high-definition multileaf collimators and fast computers enabled intensity-modulated radiation therapy, and volumetric modulated radiation therapy for stereotactic radiation therapy [Ling *et al*., 1998; Bortfeld and Schlegel, 1993]. These developments of machine quality and treatment planning computer can create more complexed and smaller radiation treatment plans and these novel techniques are available in clinic [Chun *et al*., 2017; Stahl *et al*., 2017]. These techniques can deliver high dose to tumor tissue while avoiding to critical normal tissue, but tumors in most patients recur and re-grow after radiation therapy, even after a good response at the first attempt [Coomer *et al*., 2009; Pagano *et al*., 2016]. It is difficult to improve the outcome by total dose escalation because of the normal tissue toxicity and the number of fraction limited by anesthetic risk in veterinary fields. Therefore, it is necessary to analysis biological factors related to radiosensitivity in tumors, and identify of mechanism of these factors will contribute to the improvement of radiation therapy outcome.

Cancer stem-like cells (CSCs) have attracted attention as one of the promising radio-biological factors, which play an important role of cancer survival. Bonnet and Dick [1997] were the first to identify the existence of CSCs in acute myeloid leukemia by showing that a small subset of $CD34^{+}/CD38^{-}$ cells harbored serial leukemic

transplantation potential, whereas the bulk of leukemic cells did not show this ability. Numerous studies have been performed to isolate and characterize CSCs in various kinds of human tumors, such as hepatocellular carcinoma [Yin *et al*., 2007], brain tumor [Singh *et al*., 2004], breast cancer [Ho *et al*., 2007], melanoma [Quintana *et al*., 2008], prostate tumor [Collins *et al*., 2005], gastrointestinal cancer [Haraguchi *et al*., 2006], and bone sarcoma [Murase *et al*., 2009]. Several studies have also identified canine CSCs, using several cell surface proteins and transcription factors as markers in solid tumors, including lung adenocarcinoma [Nemoto *et al*., 2011], osteosarcoma [Tanabe *et al*., 2016], mammary tumor [Michishita *et al*., 2011], mast cell tumor [Vargas *et al*., 2015], and melanoma [Inoue *et al*., 2004]. Generally, CSCs have been defined as a small subpopulation of cancer cells with peculiar molecular aspects that resemble some of typical normal stem cells, with capability of self-renewal and differentiation, and with extraordinary proliferative potential.

Several methods, including the detection of cell surface markers [Collins *et al*., 2005], side population [Murase *et al*., 2009], aldehyde dehydrogenase activity [Marcato *et al*., 2011], and a floating sphere formation [Chen *et al*. 2008], have been used to isolate CSCs from cancers and cancer cell lines. However, in veterinary fields, it is still challenging to isolate CSCs because there remain difficulty in finding cross-reacting proteins between dogs and other animals. Among the above mentioned methods, sphere formation would be particularly useful to isolate CSCs without depending on cross-reacting proteins and maintain cell viability. The sphere formation method was

established as one experimental method to identify CSCs of various cancers *in vitro* [Cao *et al*., 2011]. Only cancer cells possessing stemness or progenitor cell-like properties are able to form floating spheres under the anchorage independent condition when cultured at low density in serum-free medium containing epidermal growth factor (EGF) and basic fibroblast growth factor (FGF) [Eramo *et al*., 2008].

In vitro cell culture and animal experiments have indicated that CSCs were more resistant to radiation than non CSCs counterparts. This was clinically most important that their survival after radiation therapy might be linked to recurrence [Bao *et al*., 2006]. On the analysis on the mechanism of radio-resistance of CSCs, it has been reported that CSCs defense against reactive oxygen species (ROS) through the enhancement of glutathione synthesis [Ishimoto *et al*., 2011]. Several studies have demonstrated that CSCs possess enhanced DNA repair capacity, through especially non-homologous end-joining (NHEJ) repair capacity, in response to DNA damage by irradiation [Martins-Neves *et al*., 2012; Viale *et al*., 2009]. It has also been reported that the phosphoinositide 3-kinase (PI3K) / mammalian target of rapamycin (mTOR) signaling pathway is more activated in more aberrant manner in CSCs [Wang *et al*., 2018]. The mechanism underlying radio-resistance of CSCs is still not completely understood, especially in canine tumors. Thus, identification and elucidation of the radio-resistance mechanism of CSCs and establishment of CSCs-targeting strategy could contribute to complete cure of cancer.

For establishment of the strategies targeting CSCs, metformin would be a

candidate to potentially be used to radio-sensitize CSCs. Metformin is a biguanide derivative widely used in clinical practice as an anti-diabetic drug, but recently it has attracted attention as one of the promising anti-cancer drugs. Metformin targets the mitochondrial respiratory complex I, which leads to membrane depolarization, the release of ROS, and a decrease in the ATP/ADP ratio [Fasih *et al*., 2014; Song *et al*., 2012]. Alternatively, the inhibition of mitochondrial oxidative phosphorylation activates 5' adenosine monophosphate-activated protein kinases (AMPK) and its activation suppress the mTOR pathway, which mediates cell proliferation [Fasih *et al*., 2014]. In addition to these anti-cancer effects, recent research implicates that a role for mitochondrial complex I inhibition might be crucial for the antitumor effects of metformin [Wheaton *et al*., 2014]. Interestingly, cancers with mutation in mitochondrial genes encoding proteins of the mitochondrial complex I of the electron transport chain are more susceptible to biguanides such as metformin [Birsoy *et al*., 2014]. Unlike normal cells, cancer cells could adopt to an alternative metabolic pathway, and would exhibit enhanced glucose metabolism and production of lactate, even in the presence of oxygen [Isayev *et al*., 2014; Koppenol *et al*., 2011; Pasto *et al*., 2014]. This preferential use of anerobic glycolysis is known as the Warburg effect [Finley *et al*., 2011]. This difference in mitochondrial metabolism could explain radio-sensitivity of cancer cells, and inhibition of mitochondrial metabolism could potentially be a novel strategy to enhance radiation. The features of CSCs and their relevance in cancer therapeutics remain still unclear [Zhou *et al*., 2011]. For the establishment of novel strategy targeting

CSCs, the analysis of the radio-sensitizing effect of metformin may contribute to the elucidation of radio-resistance mechanism of CSCs.

The objectives of the present study were to elucidate the relation between the presence of CSCs and radiosensitivity of canine tumors, and to evaluate the radio-sensitizing effect of metformin for establishment of the therapeutic strategy to effecting kill CSCs by radiation. In Chapter I, spheroid cells (SCs) isolated using sphere formation were evaluated for their CSC's properties *in vitro* and *in vivo* in 4 types of canine cancer cell lines. Using colony formation assay, radio-sensitivity of SCs was tested. In Chapter II, radio-sensitizing effect of metformin was assessed in SCs derived from a canine osteosarcoma cell line. Additionally, the mechanism of radio-sensitizing effect of metformin was elucidated focusing on the inhibition of mitochondrial respiration. Here, this study demonstrates that CSCs are an important factor determining radio-sensitivity of canine cancers and providing an opportunity to develop drugs targeting CSCs, such as metformin, which inhibit mitochondrial respiration.

CHAPTER I

Analysis of radio-sensitivity of cancer stem-like cells derived from canine cancer cell lines

INTRODUCTION

Radiation therapy is an effective treatment modality for animal cancer patients. However, tumor recurrence is common after radiation therapy, despite a good response at the first intervention.

Recently, cancer stem-like cells (CSCs) have attracted attention as one of the promising radio-biological factors [Baumann and Krause, 2006; Visvader and Lindeman, 2008]. It has been reported that CSCs could be identified as a small subpopulation of self-renewing cells that generate differentiated daughter cells via asymmetric division in tumors [Coomer *et al*., 2009]. Moreover, CSCs have been thought to be resistant to cytotoxic therapy, such as radiation therapy and chemotherapy, and their survival under therapy could be linked to recurrence and metastasis of the primary tumor.

Several studies have been performed to characterize canine CSCs using several cell surface proteins and transcription factors as markers in solid tumors *in vitro*. The existence of CSCs has been reported in canine mammary tumors, showing increased expression of *CD133*, *CD34*, and *MDR*, and exhibiting drug resistance against doxorubicin [Michishita *et al*., 2011]. CSCs derived from canine lung adenocarcinoma and osteosarcoma showed greater expression of *Oct-4* and *CD133* genes, and resistance to X-ray irradiation [Tanabe *et al*., 2016]. The existence of CSCs has also been reported in canine spontaneous tumors. Tumor cells expressing *CD133*, *CD34*, *CD44*, *CD24*, and

Oct3/4 were evaluated in canine melanoma and osteosarcoma biopsy samples [Guth *et al.*, 2014]. Oct-4 expression was investigated in canine cutaneous mast cell tumors, but was not a precise prognostic factor [Vargas *et al*., 2015]. Several methods, including the detection of cell surface markers [Collins *et al*., 2005], side population (SP) [Murase *et al*., 2009; Bertolini *et al*., 2009], aldehyde dehydrogenase activity [Marcato *et al*., 2011; Michishita *et al*., 2012], and a floating sphere formation [Chen *et al*., 2008], have been employed to isolate CSCs from cancers and cancer cell lines. Sphere formation is particularly useful to isolate CSCs and maintain cell viability. Sphere-formation of CSCs was enhanced by specially designated serum-free culture medium containing several growth factors, including epidermal growth factor (EGF), fibroblast growth factor (FGF), and others [Eramo *et al*., 2008].

The sphere formation method has been commonly used to proliferate cancer cells possessing stemness property in canine solid cancers, such as those of the mammary gland carcinoma [Michishita *et al*., 2011], lung adenocarcinoma [Tanabe *et al*., 2016], and osteosarcoma [Guth *et al*., 2014]. However, stem-like cell properties, especially the radiosensitivity property of sphere-forming cells, remain unknown. The aims of this study were to isolate CSCs from canine cancer cell lines and to elucidate the relation between the presence of canine CSCs and radiosensitivity of tumor *in vitro*. In this study, sphere-forming cells derived from four canine tumor cell lines were investigated to determine whether they possess the same characteristics of CSCs, and whether they show lower radiosensitivity than their corresponding parent cells.

MATEIALS AND METHODS

Sample

Cells of a canine osteosarcoma cell line (HMPOS) [Barroga *et al*., 1999], a canine melanoma cell line (CMeC) [Inoue *et al*., 2004], a canine transitional cell carcinoma cell line (MegTCC) [Takagi *et al*., 2005; Yamazaki *et al*., 2015], and a canine lung adenocarcinoma cell line (CLAC) [Nemoto *et al*., 2011] were used in this study. Adherent cells (ACs) of HMPOS, CMeC, and MegTCC were cultured in Roswell Park Memorial Institute medium (RPMI) 1640 (Gibco by Life Techologies, Grand Island, NY, USA) supplemented with 10% fetal bovine serum (Sigma-Aldrich, St. Louis, MO, USA), 10 mM HEPES (Wako Pure Chemical Industries Ltd., Osaka, Japan), 100 units/mL of penicillin (Wako) and 100 μg/mL of streptomycin (Wako) and maintained in a humidified atmosphere with 5% CO_2 at 37℃. ACs of CLAC were cultured in Dulbecco's Modified Eagle's Medium (DMEM, Gibco), supplemented with 10% fetal bovine serum (Sigma-Aldrich), 10mM HEPES (Wako), 100 units/mL of penicillin (Wako) and 100 μg/mL of streptomycin (Wako) and maintained in a humidified atmosphere with 5% CO_2 at 37℃.

Sphere formation

When cells reached approximately 70%-80% confluency in adherent culture condition, cells were detached by 0.25% trypsin-ethylenediaminetetraacetic acid

(EDTA) (Wako). Cells were cultured in ultra-low attachment 6-well plates (Corning, Corning, NY, USA) at a density of 1×10^4 cells per well. These cells were incubated in serum-free DMEM/F12 (Wako) supplemented with 0.4% bovine serum albumin (Invitrogen Life Technologies, Carlsbad, CA, USA), 5 mM HEPES, 100 units/mL of penicillin, 200 mg/mL of streptomycin, 20 ng/mL of human recombinant EGF (Wako) and 10 ng/mL of human recombinant basic FGF (Wako) and maintained in a humidified atmosphere with 5% CO_2 at 37°C. The medium was daily supplemented with 2 ng/mL of EGF and 1 ng/mL of bFGF for 14 days. Spheroid cells (SCs) of > 50 μm were collected under low magnification and suspended to form a single-cell suspension using 0.25% trypsin-EDTA (Wako). Thereafter, SCs were counted and used for the following analyses.

Reverse transcription-polymerase chain reactions (RT-PCR)

Each AC was collected when cells reached approximately 70%-80% confluent. Each SC was collected at 14 days of sphere formation. Total mRNA was extracted from the cells using the TRIZol® reagent (Invitrogen) according to manufacturer's protocol. The quantification of total RNA was performed using spectrophotometry at 260 nm. A total of 500 ng of RNA was reverse-transcribed into cDNA using the M-MLV RT kit (Invitrogen) according to manufacturer's protocol, and PCR amplification was performed using TaKaRa Ex taq® (TaKaRa Bio, Kusatsu, Japan). The PCR conditions were an initial denaturation of 94°C for 1 minute followed by 35 cycles of 94°C for 30

seconds, 58°C for 30 seconds, and 72°C for 30 seconds, and then a finishing step of 72°C for 1 minute. Gene expression was visualized using 1 % agarose gel electrophoresis. The sequences of primers used for RT-PCR are shown in Table I-1. Detectable bands were measured using Image J (National Institutes of Health, Bethesda, MD, USA) software.

Xenografts in nude mice

In this study, 7-week-old female BALB/cAJc1 nu/nu mice (Hokudo Co., Ltd, Sapporo, Japan) were used in accordance to the Hokkaido University Institutional Animal Care and Use Committee guidelines (approval number: 17-0044). As previously described, ACs and SCs of 4 cell lines were collected. Cells were prepared at 1×10^2 (HMPOS and CLAC) or 1×10^3 (CMeC and MegTCC) cells in 50 µl of phosphate-buffered saline (PBS, pH 7.4). Before injecting into mice, cells were mixed with 50 µl of Matrigel® (BD Bioscience, San Jose, CA, USA). The mixture of cells in Phosphate buffered salts (PBS) and Matrigel was subcutaneously injected into the dorsal region of mice. Until the end of assessment period (16 weeks or tumor volume > 2×10^3 mm^3), it was daily measured tumor volume (tumor volume=length × $[width]^2$ × 0.5). At the end of the assessment period, mice were humanely sacrificed using inhalation of CO_2 gas and tumors were resected. The tumors were fixed with 10% buffered formalin, embedded in paraffin, cut into 3 µm sections, and stained using hematoxylin and eosin (HE).

X-ray irradiation

X-ray irradiation for cells was performed using the X-ray generator, X-RAD® iR-225 Xray irradiator (Precision X-Ray, North Branford, CT, USA) with a dose rate of 1.37 Gy/min at 200 kVp and 15 mA, with a 1.0 mm aluminum filter at room temperature (RT).

Clonogenic survival assay

As previously described, ACs and SCs of 4 cell lines were collected. Cells were plated at various concentrations in 60 mm diameter dishes and cultured for 6 hours similar to the adherent culture condition. The cells were then X-ray irradiated and the medium was changed to fresh medium. After incubation for 7 days, cells were fixed with methanol and stained with the Giemsa solution (Wako). Each colony that consisted of > 50 cells was scored as colony forming cell, and the plating efficiency (PE) was then calculated. Survival fractions were calculated with a correction for PE of the unirradiated control, and dose-response curves were plotted. Three independent experiments were carried out, and survival curves were then fitted to a linear-quadratic model: $SF = (-\alpha D-\beta D^2)$, where SF was the surviving fraction and D indicates the physical dose.

Immunofluorescence staining for p53-binding protein 1

As previously described, ACs and SCs of 4 cell lines were collected. Cells were

seeded in a slide and cultured for 6 hours. After 1 Gy of X-ray irradiation for the indicated time, cells were fixed with 4% paraformaldehyde (Wako) for 20 minutes at RT followed by permeabilization with PBS containing 0.5% Triton X-100 (ICN Biomedicals, Irvine, CA, USA) for 5 minutes at 4°C and then blocked with PBS containing 6% goat serum (Wako) for 30 minutes at RT. After blocking, cells were washed three times with PBS, and the cells were probed with a rabbit anti- p53-binding protein 1 (53BP1) antibody (Abcam Inc., Cambridge, UK) at 1:2,000 dilution in 3% goat serum overnight at 4°C. After washing three times with PBS, cells were stained with an Alexa Fluor 488-conjugated anti-rabbit secondary antibody (Abcam.) at a 1:2,000 dilution for 90 minutes in the dark at RT. To counterstain nuclei, cells were mounted with Prolong® Diamond Antifade Mountant with 4', 6'-diamidino-2-phenylindole (DAPI; Thermo Fisher Scientific, Waltham, MA, USA). Fluorescence of 53BP1 and nuclei was detected with an Olympus BX50 microscope (Olympus, Tokyo, Japan), and the number of 53BP1 foci per cell was counted using Image J software.

Statistical analysis

All results are represented as mean ± standard deviation (SD). For statistical analysis, JMP® 14 (SAS Institute Inc., Cary, NC, USA) software was used. The sphapiro-wilk test was used to determine whether the values were normally distributed. The non-parametric tests were used in case the values were not normally distributed or if sample size was small. Significance of difference for the survival curve and DNA

kinetics between ACs and SCs was tested using the Mann-Whitney *U* test. Student's *t*-test was performed to analyze significant differences for the other date between ACs and SCs. Those resulting in p values <0.05 were considered statistically significant.

Table I-1 Primer pairs used for RT-PCR

Gene	Forward primer 5’-3’	Reverse primer 5’-3’
GAPDH	CTGAACGGGAAGCTCACTGG	CGATGCCTGCTTCACTACCT
CD133	GCTGCTCTTTGTGATTCTGATG	ATCACCAGGAGGGAGACTGTAA
Oct-4	CTCTGCAGCCAATCAACCACAA	GGGAGAGGGGATGAGAAGTACAAT
Sox-2	AACCCCAAGATGCACAACTC	CGGGGCCGGTATTTATAATC
c-myc	AATAGGAACTATGACCTCGAC	AGCAGCTCGAATTTCTTCCAG
CD34	TGAGACCTCCAGCTGTGA	CAGGTGTTGTCTTGCTGAATGG
CD44	AATGCTTCAGCTCCACCTG	CGGTTAACGATGGTTATGGTAATT
Stat3	GTGGAGAAGGACATCAGCGGTAA	AACTTGGTCTTCAGGTATGGGGC
MDR	GAGGACTTGAATGAGAATGTTCCT	CGGGTAAAGATCCCTATAATCCTT
Notch1	AGGACCGTGACAATGCCTAC	ACACTCGTAACCGTCGATCC
MELK	CCAAGGGTAACAAGGACTAC	CTCCAAACATCTGCCTCTGA

RESULTS

Sphere formation

After 14 days of incubation, all four cell lines formed spheres. Morphological characteristics of each sphere were similar to each other (Figure I-1A-D). The number of spheres (mean ± SD) of HMPOS, CMeC, MegTCC, and CLAC were 55.33±4.36, 46.27±2.13, 42.67±2.16 and 42.17±3.06, respectively. Only few spheres were detected in all four cell lines under the culture conditions without growth factors (Figure I-1E).

Expression of CSC markers in ACs and SCs

To evaluate the expression of mRNAs of CSC marker genes (*CD133, Oct-4, Sox-2, c-myc, CD34, CD44, Stat3, MDR, Notch1,* and *MELK*), SCs were analyzed by RT-PCR and compared with those of AC. As shown in Figure II-2 A and B, the expressions of *CD133, Oct-4, c-myc, CD34, CD44, Stat3, MDR, Notch1,* and *MELK* (HMPOS), *CD133, Oct-4, Sox-2, c-myc,* and *MDR* (CMeC) , *CD133* and *CD34* (MegTCC), and *CD133, Oct-4, CD44, Stat3, MDR, Notch1,* and *MELK* (CLAC) were significantly higher in SCs than ACs. Additionally, SCs of all four cell lines showed markedly high expression of *CD133*, but it was almost undetectable in AC of all four cell lines.

Tumorigenic capacity of ACs and SCs

The tumorigenic capacity of ACs and SCs was evaluated using xenografts in nude mice and varying number of these cells was subcutaneously injected into nude mice. Then, 24 days after transplantation, the tumor volume of the three mice transplanted with SCs of HMPOS reached 2×10^3 mm^3, and mice transplanted with SCs and ACs of HMPOS were humanely sacrificed. At the end of the assessment, solid tumors were observed in four mice transplanted with SCs of HMPOS, whereas no solid tumors were observed in mice transplanted with the ACs of HMPOS. Moreover, 112 days after transplantation, all other mice were humanely sacrificed using inhalation of CO_2 gas. Solid tumors were observed in two of four mice transplanted with SCs of MegTCC, whereas no solid tumors were observed in mice transplanted with corresponding ACs. Solid tumors were observed in four mice transplanted with SCs of CMeC and CLAC, whereas solid tumors were observed only in three and two of four mice transplanted with corresponding ACs of CMeC and CLAC, respectively. In HMPOS and MegTCC, SCs had significantly higher tumorigenic ability but not in CMeC and CLAC. Additionally, the volume of tumors derived from SCs was approximately 10 times higher than those from ACs. The difference of tumor volume between ACs and SCs was statistically significant in CMeC (p=0.0304) but not in CLAC (p=0.2472). These tumors were all histopathologically diagnosed as same as original tumor type. (Figure I-3 1 and 2). (Table I-2)

Clonogenic survival following exposure to X-irradiation

Each SC and AC of all four cell lines were irradiated with 0, 2.5, 5.0, 7.5, and 10 Gy of X-ray, and colony formation was measured. The viability of all cells reduced in a dose-dependent manner at 7 days after X-ray irradiation. All SCs of the four cell lines showed significant resistance against X-ray irradiation of each dose compared with ACs (Figure I-4). Each cell was characterized by PE, survival fractions of 2.5, α, β, and α/β ratio, with the date summarized in Table I-3. PE of SCs was significantly higher than those of ACs in all four cell lines. The α/β ratio of SCs (1.52-3.18 Gy) was lower than that of ACs (3.94–8.34 Gy) in all four cell lines (Table I-3).

DNA double-strand breaks of ACs and SCs following exposure to X-ray irradiation

To investigate the kinetics of DNA double-strand break (DSB) rejoining, 53BP1 foci were measured at 0.5, 1, 2, 4, and 6 hours after X-ray irradiation (1 Gy) in ACs and SCs of the four cell lines. The average number of 53BP1 foci per cell was about the same in all non-irradiated cells. In both SCs and ACs of all four cell lines, the average number of foci per cell peaked at 0.5 hour post irradiation, with the exception of SCs of CMeC (peak was at 1 hour). The number of foci slowly decreased and remained higher than pre-irradiation for approximately five at 6 hours post irradiation in ACs and SCs of all four cell lines. However, the peak number of foci in SCs of the four cell lines was significantly lower than that of ACs. (Figure I- 5 and 6)

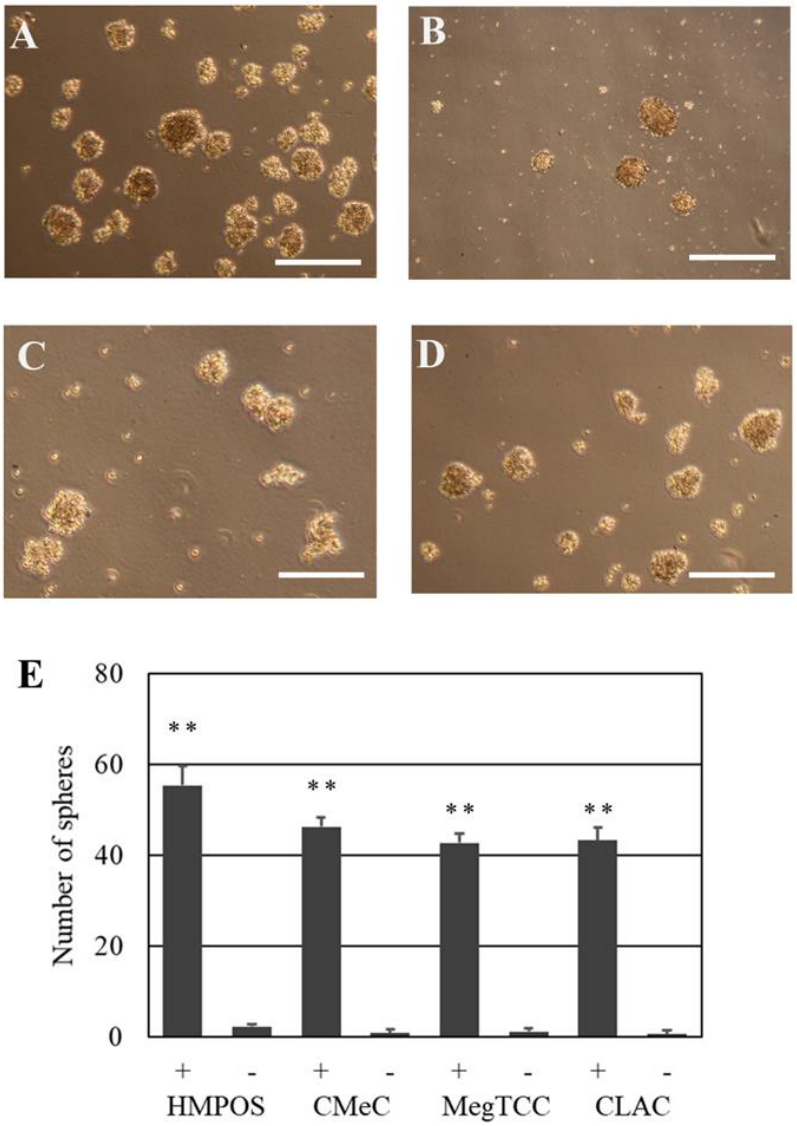

Figure I-1. Spheres of HMPOS (A), CMeC (B), MegTCC (C), and CLAC (D).

The data are represented as a mean ± S.D. Evaluation of the number of spheres from the all four cell lines (E). Cells were grown in serum-free medium supplemented with (+) or without (-) growth factors for 14 days. These results were analyzed using Student's *t*-test. *$p < 0.05$ and **$p < 0.01$ for ACs versus SCs. Bar = 300 μm.

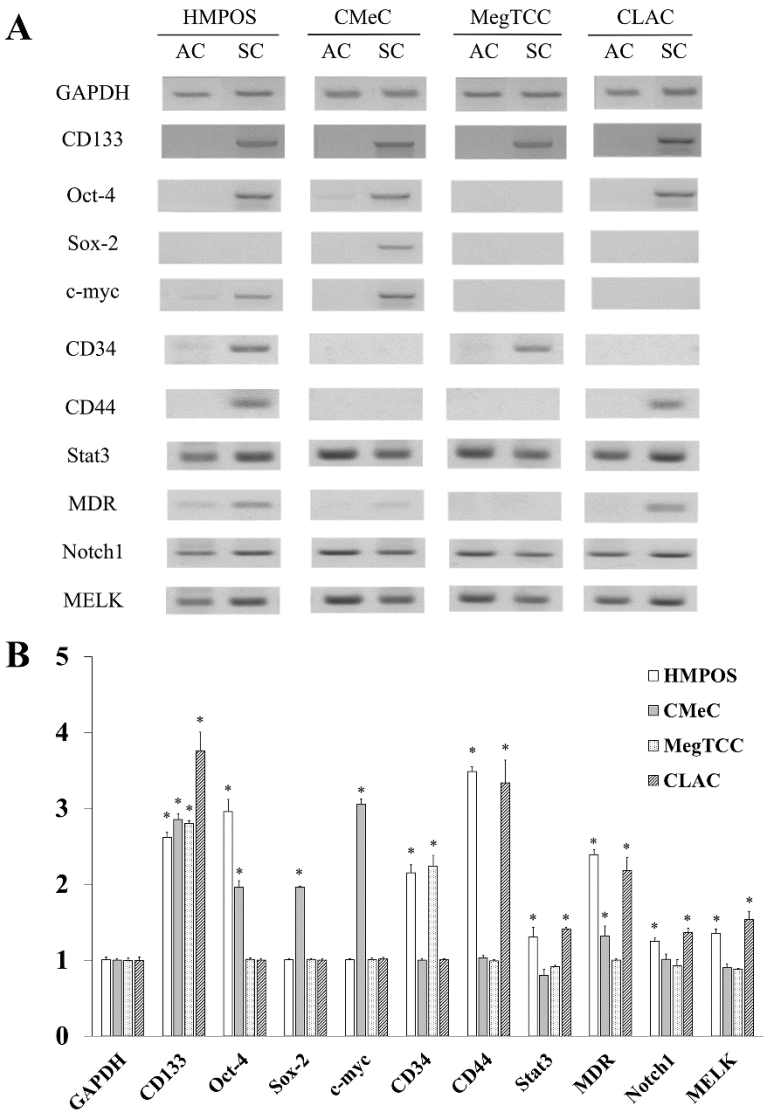

Figure I-2. Expression of GAPDH, CD133, Oct-4, Sox-2, c-myc, CD34, CD44, Stat3, MDR, Notch1, and MELK genes.

CSCs-like properties, such as the upregulation of stemness markers, were evaluated in ACs and SCs (A). Semiquantitative analysis of the mRNA expression (B). The index of expression was defined as the ratio of SCs to ACs. Results are indicated as means ± SD of at least three experiments. Statistical analysis was performed using Student's *t*-test. *$p < 0.05$ versus GAPDH.

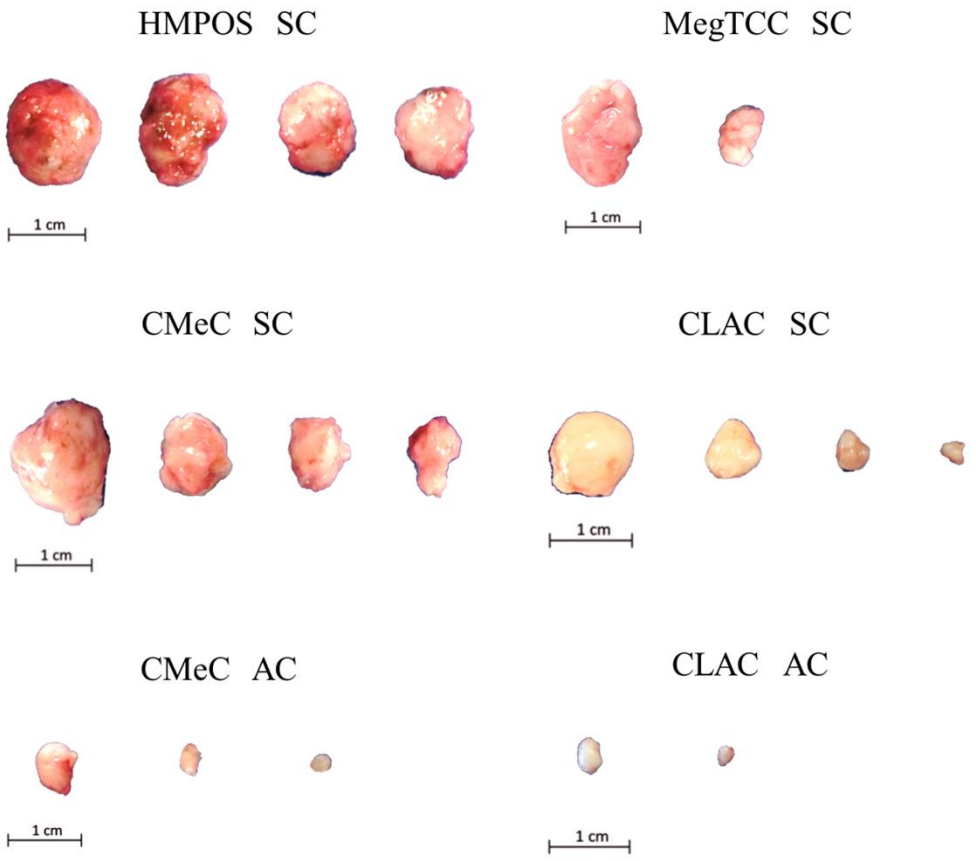

Figure I-3-1. Tumorigenesis of ACs and SCs

Tumor of SCs derived from HMPOS, CMeC, MegTCC, and CLAC and ACs derived from CMeC and CLAC (ACs of other two cell lines did not form a tumor). Tumors were observed in four and two mice transplanted with SCs of HMPOS and MegTCC, whereas no solid tumors were observed in mice transplanted with the ACs. Tumors were observed in four mice transplanted with SCs of CMeC and CLAC, whereas solid tumors were observed only in three and two of four mice transplanted with corresponding ACs of CMeC and CLAC, respectively.

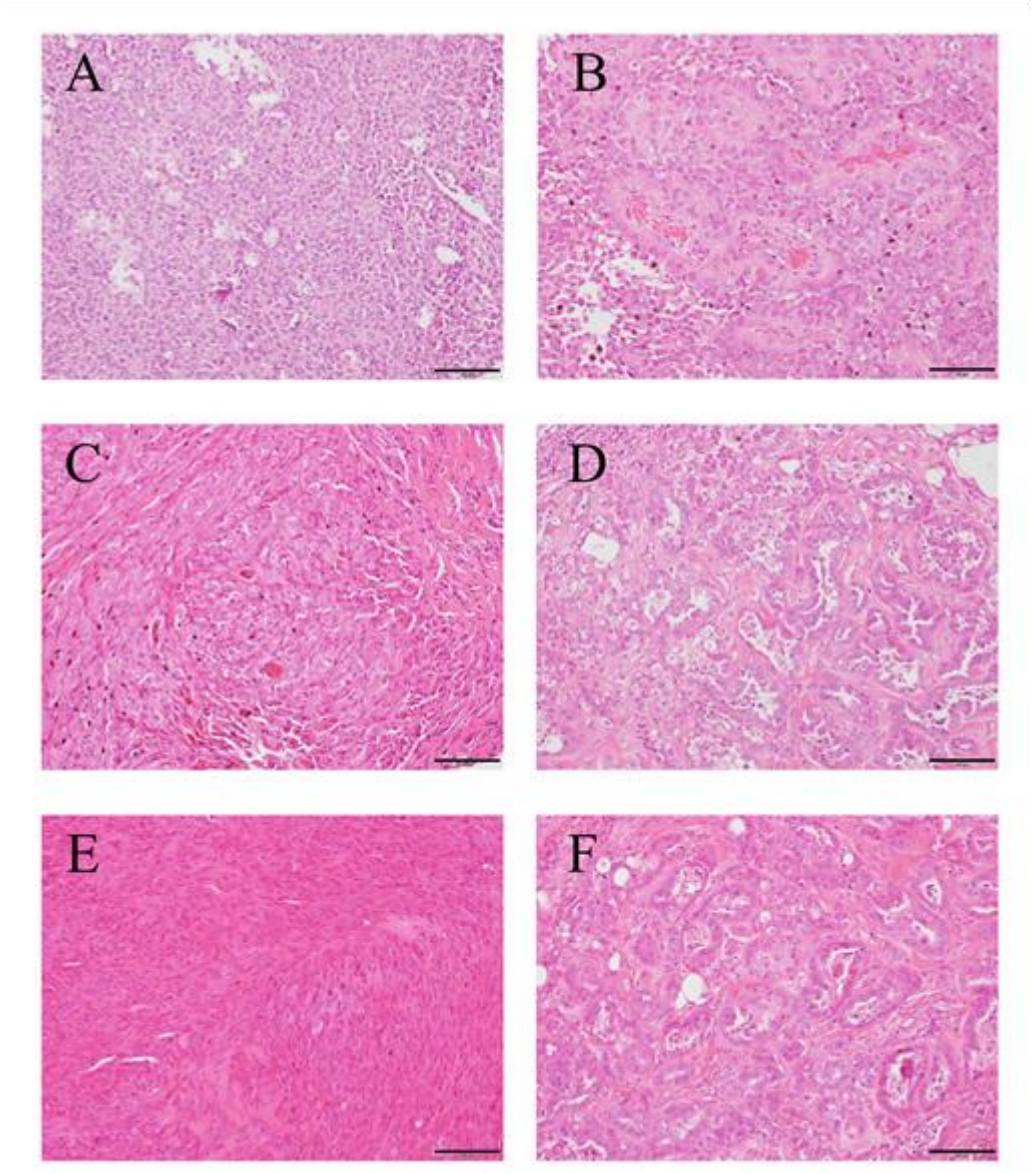

Figure I-3-2. Histopathology of the xenografted tumor of ACs and SCs

Histopathology of the xenografted tumor derived from SCs of HMPOS (A), MegTCC (B), CMeC (C), and CLAC (D) and ACs derived from CMeC (E) and CLAC (F), haemotoxylin and eosin (HE) staining (×200). Bar = 100 μm.

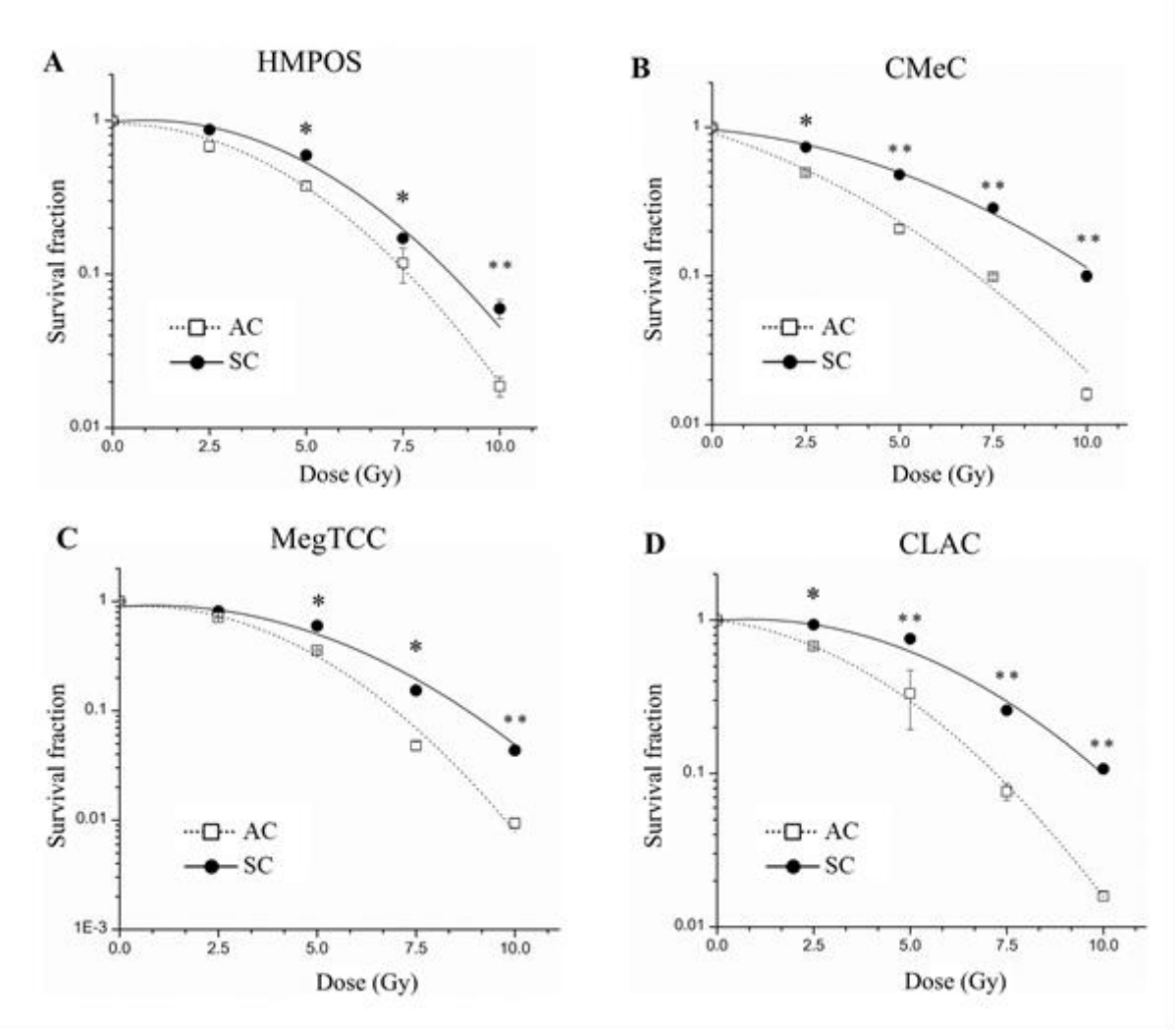

Figure I-4. Survival curves of ACs and SCs in the four canine tumor cell lines.

Evaluation of radiosensitivity by clonogenic assay in ACs (□) and SCs (●)of HMPOS (A), CMeC (B), MegTCC (C), and CLAC (D). The data are represented as means ± SD from independent three experiments. These results were analyzed using Mann-Whitney *U* test. **p* < 0.05 and ***p* < 0.01 for ACs versus SCs.

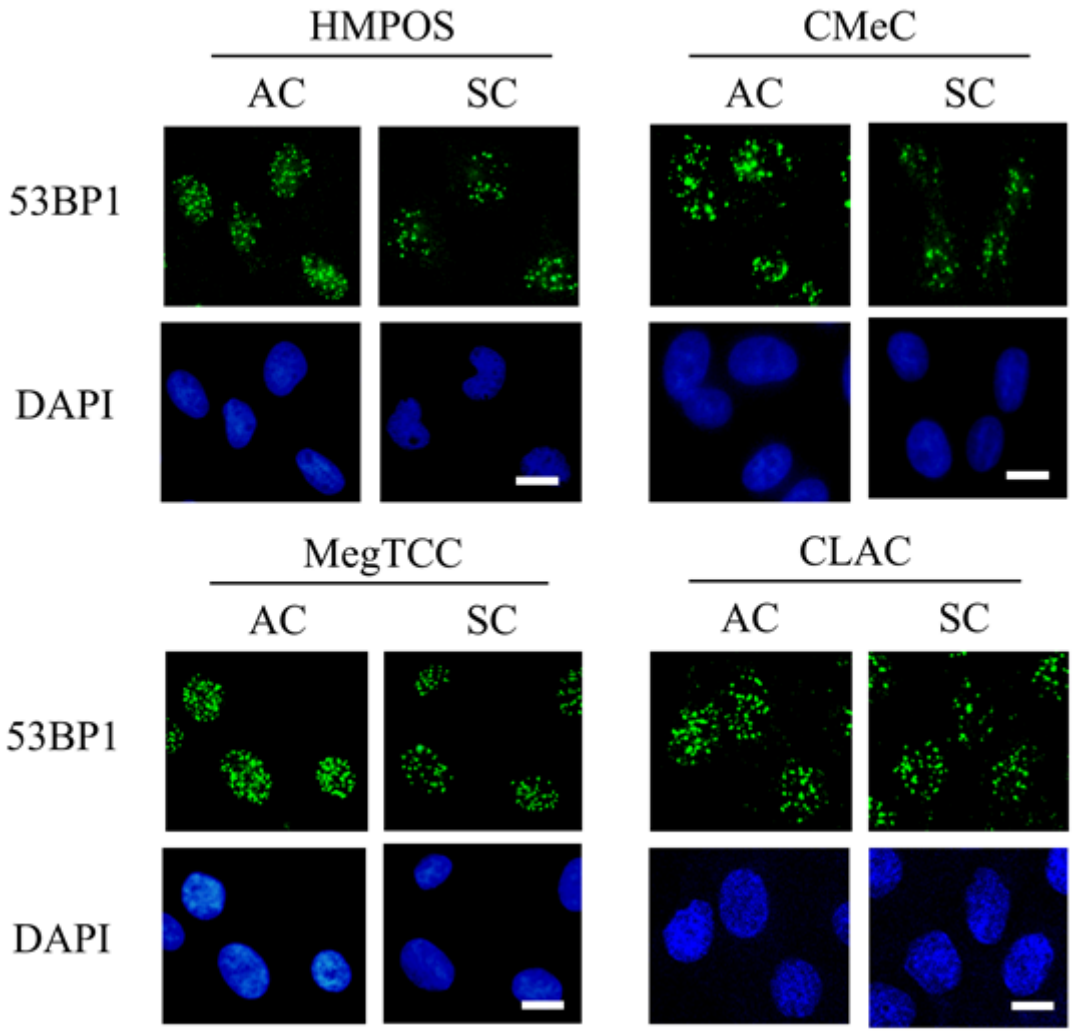

Figure I-5. Images of p53-binding protein 1 (53BP1) foci after irradiation.

Representative images of 53BP1 foci in 4', 6'-diamidino-2-phenylindole (DAPI)-treated ACs and SCs of HMPOS, CMeC, MegTCC, and CLAC at 30 minutes after X-ray irradiation (1 Gy).

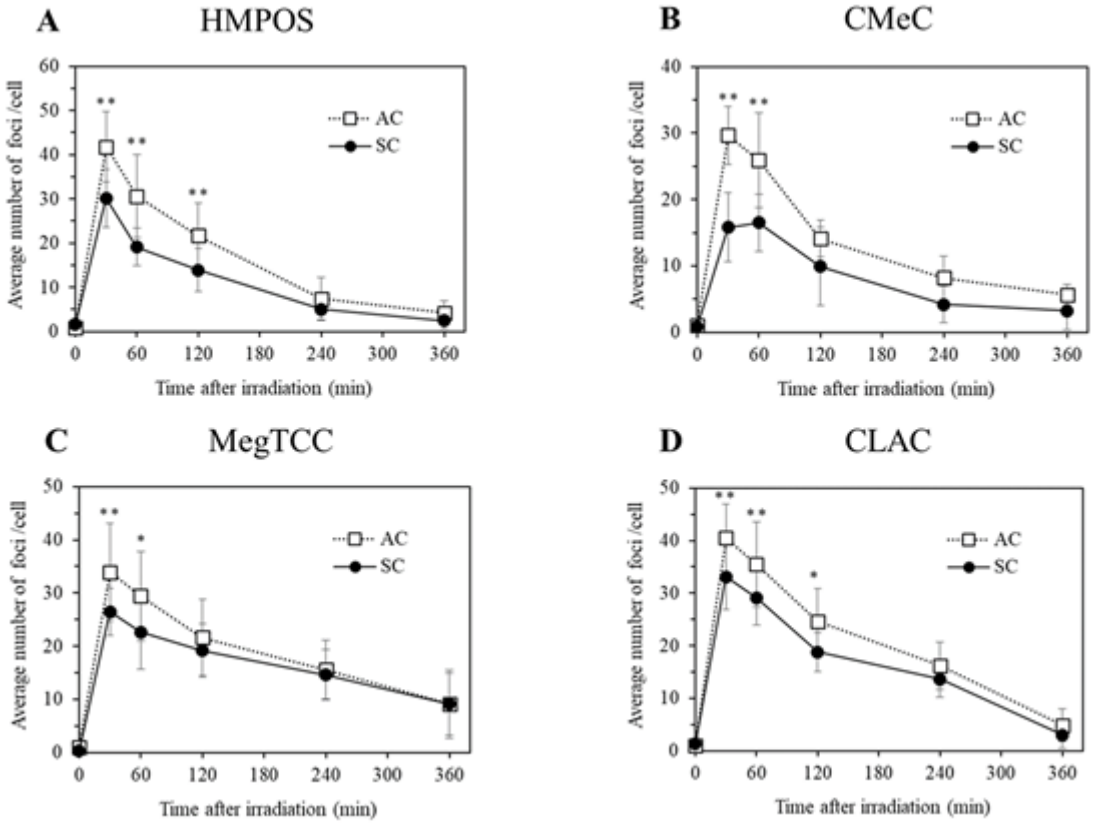

Figure I-6. DNA repair kinetics after X-ray irradiation.

Analysis of DNA repair kinetics for the formation of 53BP1 foci in ACs (□) and SCs (●) of HMPOS (A), CMeC (B), MegTCC (C), and CLAC (D). After 1 Gy X-ray irradiation, quantitative assessment for number of 53BP1 foci in at least 50 cells at the 0.5, 1, 2, 4, and 6 hours, were scored and the average numbers of foci were plotted. The data are represented as means ± SD. from independent three experiments. These results were analyzed using Mann-Whitney U test. *$p < 0.05$ and **$p < 0.01$ for ACs versus SCs.

Table I-2. Tumorigenesis of the ACs and SCs derived from HMPOS, CMeC, MegTCC, and CLAC.

Cell line		Cell number	Tumorigenesis	Tumor Volume (mm3)	Days
HMPOS	SC	1×10^2	4/4	1865.4 ± 155.8	24
	AC	1×10^2	0/4	-	24
CMeC	SC	1×10^3	4/4	958.9 ± 620.7	112
	AC	1×10^3	3/4	93.6 ± 92.1	112
MegTCC	SC	1×10^3	2/4	1158.5 ± 1151.4	112
	AC	1×10^3	0/4	-	112
CLAC	SC	1×10^2	4/4	557.2 ± 241.5	112
	AC	1×10^2	2/4	17.4 ± 28.5	112

Tumor volume (mm^3) represents means ± SD of four mice.

Table I-3. Values of radiobiological parameters in ACs and SCs of four cell lines.

Cell line		PE	SF 2.5	α	β	α/β ratio
HMPOS	SC	0.44 ± 0.04	0.59 ± 0.03	0.055	0.036	1.52
	AC	0.39 ± 0.04	0.41 ± 0.06	0.083	0.019	4.36
CMeC	SC	0.16 ± 0.01	0.47 ± 0.03	0.051	0.016	3.18
	AC	0.09 ± 0.03	0.20 ± 0.01	0.155	0.023	6.74
MegTCC	SC	0.36 ± 0.02	0.58± 0.01	0.058	0.034	1.71
	AC	0.26 ± 0.02	0.33 ± 0.01	0.367	0.044	8.34
CLAC	SC	0.49 ± 0.02	0.75 ± 0.01	0.044	0.027	1.62
	AC	0.40 ± 0.01	0.33 ± 0.02	0.071	0.018	3.94

PE: Plating efficiency, SF 2.5: survival fraction 2.5Gy, and, α, β, and α/β ratios: value were derived from survival curves fitted to a linear-quadratic model ($SF = -\alpha D-\beta D^2$), where SF was the surviving fraction and D indicates the physical dose. Date are represented as means ± SD.

DISCUSSION

Sphere formation is one of methods to isolate CSCs from cancers. The principle of sphere formation has not been completely understood. It was demonstrated that spheres formed well in non-adherent conditions in serum-free medium in the presence of growth factors in canine neoplastic cell lines. Ultra-low attachment condition may limit normal cell growth, proliferation, and differentiation by inhibiting the attachment to extracellular matrix [Frisch and Francis, 1998; Ruoslahti and Reed, 1994]. Additionally, EGF signaling is activated by EGF receptors and thought to be important in the maintenance of the stemness properties [Soeda *et al*., 2008]. FGF is also known to play an important role in sphere formation [Kondo *et al*., 2004].

CD133 expression was reported to be associated with the prognosis of human osteosarcoma [Tirino *et al*., 2011], lung cancer [Mizugaki *et al*., 2014], colon cancer [Ricci-Vitiani *et al*., 2007], and glioma [Singh *et al*., 2004]. The function of CD133 in cancer cells might play an important role in asymmetric cell division, initiation of cancer, and higher DNA repair capacity [Bao *et al*., 2006; Viale *et al*., 2009]. It was demonstrated that SCs derived from various tumor cell types, including osteosarcoma, melanoma, transitional cell carcinoma, and lung adenocarcinoma, markedly expressed *CD133*, suggesting that the SCs used in this study possessed stemness. However, at the protein level, it was not able to detect CD133 in spite of using several different mouse antibodies against CD133 (data not shown) because these antibody could not cross-react

in four cell lines. The genomic structure of mammalian *CD133* is strikingly similar and remarkably conserved across species [Fargeas *et al*., 2003]. Despite this genomic feature, the amino acid sequence is poorly conserved among CD133 gene products, especially C-terminal domain [Han and Pepermaster, 2011; Jaszai *et al*., 2011]. The low level of amino acid conservation of CD133 between species may explain the lack of cross-species immunoreactivity of specific CD133 antibodies between canine and mouse proteins [Thamm *et al*., 2016]. Further analysis is necessary to detect CD133 protein expression in canine CSCs.

Other genes, such as *Oct-4*, *Sox-2*, *Notch1*, and *c-myc*, are associated with the maintenance of stem cells [Takahashi and Yamanaka, 2006]. ATP-binding transporters, such as MDR, were discovered as proteins overexpressed in drug-resistant cancer cell lines. MDR may be involved in the efflux capacity of the side population of tumor cells that is enriched in stem cells [Goodell *et al*., 1996]. It has also been reported that spheroid cells derived from canine mammary gland adenocarcinoma cell lines show high *MDR* expression and are resistant to doxorubicin [Michishita *et al*., 2011]. Expression of the *MDR* gene in SCs is related to chemo-resistance and hence probably to treatment failure.

In this study, we detected the highly tumorigenic capability of SCs compared to ACs using xenograft model except for CLAC. It has been demonstrated that 1×10^5 – 5×10^6 cells are generally used to generate a tumor with non-CSCs, or ACs [Nemoto *et al*., 2011; Wang *et al*., 2014]. In CSCs, on the other hand, SCs derived from canine

mammary gland carcinoma, lung adenocarcinoma, and osteosarcoma [Tanabe *et al*., 2016] formed tumors with the inoculation of cells as few as 1×10^2. In the present study, only 1×10^2 and 1×10^3 of SCs formed tumors, suggesting that these cells isolated by sphere formation method had the high tumorigenic capacity, one of the characteristics of CSCs. However 1×10^3 ACs of CMeC and 1×10^2 ACs of CLAC formed tumors in this study. Tanabe *et al*. [2016] demonstrated that 1×10^2 ACs of CLAC also formed tumors. Therefore, it has been suggested that CLAC has a highly tumorigenic ability even as ACs. Furthermore, tumor volume of SCs was larger than ACs and this result also suggested that SCs had high tumorigenic ability. However, tumor volume between ACs and SCs was not significantly different in CLAC. The statistical power is very low ($\beta = 0.1649$), but in CLAC larger sample number may be needed than used in our study.

In this study, SCs of all four types of canine cancer showed radio-resistance compared to those of ACs determined by clonogenic assay. It has been reported that human CD133-positive glioblastoma CSCs are more resistant to X-ray irradiation than CD133-negative cells. Tanabe *et al*. [2016] demonstrated SCs had radio-resistance in canine lung adenocarcinoma and osteosarcoma determined by 3-[4, 5-dimethylthiazol-2-yl]-2, 5 diphenyl tetrazolium bromide (MTT) assay. These results suggests that radio-resistance of canine cancer is, at least in part, caused by the presence of CSCs. Additionally, clonogenic assay is a more widely used method to evaluate proliferative capability of cells after the treatment with ionizing radiation than MTT assay, which is

used to simply assess cell viability through mitochondrial activity.

The kV machine, which delivered the dose at the rate of 137 cGy/min, was used in this study. It is now possible to perform irradiation at a dose rate higher than 400 cGy/min using a linear accelerator. However, it was considered that the dose rate of 137 cGy/min was more appropriate, since intensity-modulated radiation therapy creates a very complicated irradiation field and takes more time to deliver the dose to the target (with the effective dose rate of around 200 cGy/min or less, depending on the degree of modulation and complexity of the plan) [Dolera *et al*., 2018]. Furthermore, increment of dose rate of 200 to 400 cGy affects only less than 1% for cellular survival fraction. The difference in these dose effect to survival fraction between 100 and 1000 cGy/min is very small [Ling *et al*., 1998].

The α/β ratio has been used as a parameter of tissue radio-sensitivity, specifically the effect of a fractionation schedule on cell survival. Early-responding tissues (e.g., skin and mucosa) and tumors have high α/β ratio (usually 7-20 Gy, with an average of about 10 Gy), whereas late-responding tissues (e.g., brain, spinal cord, and kidneys) have low α/β ratio (usually 1-6 Gy, with an average of about 3 Gy) [Williams *et al*., 1985]. However, as exceptions, a few tumors are known to have a low α/β ratio, such as a prostate cancer (1.5 Gy) [Brenner and Hall, 1999], and theoretically more likely to survive conventionally fractionated radiation therapy than tumors with a high α/β ratio. In this study SCs of the all four cell lines were shown to have significantly lower α/β ratios (range: 1.52-3.18 Gy) than those of ACs (range: 3.94-8.34 Gy). This

results suggest that CSCs of canine cancer are resistant to conventional fractionated radiation therapy (larger numbers of smaller fractions), and that hypofractionated radiation therapy, such as the fractionation currently used in stereotactic radiation therapy (smaller numbers of larger fractions), is more effective in controlling CSCs of canine cancers.

X-ray radiation induces DSBs after X-ray exposure, DSBs can be repaired by NHEJ and homologous recombination repair in the condition where the sister chromatid can serve as a template [Schipler and Iliakis, 2013]. Repair of lesions of DSBs accumulate 53BP1 in large segments of lesion-flanking chromatin that can be observed with fluorescence microscopy as nuclear foci [Lukas *et al*., 2011]. Therefore, 53BP1 foci are useful markers for DSB induction and repair [Martin *et al*., 2013]. On the analysis of DNA kinetics, the peak number of foci indicates the reactive oxygen species (ROS) scavenging ability and the rate of time dependent reduction of the number of foci relates DNA repair capacity. In this study, the peak foci number in SCs of all four cell lines were significantly lower than those in ACs. These results suggest that radio-resistance of CSCs were related to highly ability of ROS scavenging after X-ray exposure. On the analysis of mechanism of radio-resistance of CSCs, CSCs have an enhanced capacity for glutathione synthesis and defense against ROS [Ishimoto *et al*., 2011]. Approximately 70% of the biological damage produced by X-ray is through indirect action, which involves the ionization of water molecule producing ROS, which in turn combines with the damaged DNA. It showed that SCs had lower number of

DNA DSBs after X-ray irradiation and it may suggest that SCs have a high ability to suppress intracellular ROS formation or scavenge ROS. However, several studies have demonstrated that CSCs possess enhanced DNA repair capacity [Martins-Neves *et al*., 2012; Viale *et al*., 2009]. CSCs exhibit increased DNA repair activity, through elevated NHEJ levels, in response to DNA damage, which may have been caused by irradiation [Chang *et al*., 2015]. It could not be ruled out that rapid DNA repair affected the decrease in the peak number of foci.

In conclusion, results of present study suggest that SCs isolated using sphere formation had CSC-like properties and radio-resistance in several types of canine tumors. Further studies are required for the elucidation of CSC radio-resistance mechanism to better target CSCs.

SUMMARY

Cancer stem-like cells (CSCs) are self-renewing cells comprising a small subpopulation in tumors, and generate differentiated progeny via asymmetric division. It has been shown that CSCs are resistant to ionizing radiation, and this feature could be one of the mechanisms of tumor recurrence after radiation therapy. Much attention has been paid on to target CSCs, but, the difficulty in isolating CSCs and lack of knowledge on their radiosensitivity have limited this kind of research in veterinary medicine. In this study, spheroid cells (SCs), cultured using sphere formation method, were isolated from four type of canine tumor cell lines and determined if they have CSCs-like properties. All SCs were isolated by using sphere formation and showed high *CD133* expression and tumorigenic ability compared to adherent cells (ACs). All SCs were significantly resistant against X-ray irradiation compared to ACs. In addition, the amount of DNA double strand breaks after X-ray irradiation were significantly lower in SC compared to the corresponding ACs. These results showed that SCs isolated via sphere formation possess CSCs-like characteristics and CSCs are important factor that affect radiosensitivity in canine tumors. In addition, radio-resistance of CSCs may depend on the reaction of DNA double strand breaks, such as the decrease in the peak number and rapid repair of DNA after X-ray exposure.

CHAPTER II

Metformin preferentially enhances the radiosensitivity of cancer stem-like cells with high mitochondrial respiration ability in a canine osteosarcoma cell line

INTRODUCTION

Solid tumors are composed of heterogeneous cancer cells and contain a small subpopulation of CSCs [Eramo *et al*., 2008]. It has been demonstrated CSCs are characterized to be self-renewing cells in tumors that generate differentiated progeny by the differentiation to CSCs and non-CSCs, and unlimited proliferative capacity [Visvader and Lindeman, 2008]. Several studies have indicated that CSCs are more resistant to radiation therapy than non-CSCs and their survival after radiation therapy has been linked to cancer recurrence [Baumann and Krause, 2010]. In chapter I, it was also demonstrated SCs derived from canine cancer cell lines had a radioresistance compared to ACs. This result suggested CSCs is one of the important factor to determine radiosensitivity in canine tumors.

Recently, metformin has gained attention as one of the promising anti-cancer drugs which can enhance tumor cells' (especially CSCs) radiosensitivity [Samsuri *et al*., 2017; Song *et al*., 2012]. Metformin targets the mitochondrial respiratory complex 1, which leads to membrane depolarization, release of ROS, and decrease in oxygen consumption, decrease in mitochondrial membrane potential, and decrease in the ATP/ADP ratio [Rena *et al*., 2017]. Inhibition of mitochondrial complex and changing energy depletion activates 5' adenosine monophosphate-activated protein kinases (AMPK), which suppress the mTOR pathway [Rocha *et al*., 2018]. However, the results of radio-enhancement mechanism by metformin are controversial, especially in the case

of CSCs. For example, Lonardo *et al*. [2013] showed that metformin's effect mostly relied on the inhibition of mitochondrial function, which apparently is lethal for CSCs both *in vitro* and *in vivo*. However, Song *et al*. [2013] showed that metformin and ionizing radiation activated AMPK leading to the inactivation of mTOR and suppression of its downstream effectors on CSC. The mechanism of metformin through which it radio-sensitizes CSCs remains an area of active investigation. Moreover, metformin was more effective against cells having a higher mitochondrial respiration level. However, the factors determining radio-sensitizing effect of metformin has not been elucidated to date.

This study determined the radio-sensitization effects of metformin both *in vitro* and *in vivo*, including the investigation of its radio-sensitization mechanism and difference in radio-sensitizing efficiencies between SCs and their parental ACs. Metformin preferentially radio-sensitized SCs leading to the inhibition of mitochondrial respiration, but not to AMPK activation. Additionally, SCs had a higher ability of mitochondrial respiration than ACs; it might cause the difference in radio-sensitizing effect of metformin. In summary, mitochondrial respiration might play a central role in the radio-resistance mechanism of CSCs and metformin is a promising radio-sensitizer that can inhibit mitochondrial respiration of CSCs.

MATERIALS AND METHODS

Reagents and treatment

Metformin hydrochloride (metformin), rotenone, carbonyl cyanide m-chlorophenyl hydrazine (CCCP), and oligomycin were obtained from Wako Pure Chemical Industries. The X-ray irradiation was performed using X-ray generator TITAN-320S (Shimadzu Industrial System Co., Ltd., Kyoto, Japan) with a dose rate of 4.17 Gy/min at 200 kVp and 20 mA, using a 2.0 mm aluminum filter at RT.

Cell culture

The canine osteosarcoma cell line HMPOS was used in this study [Barroga *et al.* 1999]. ACs were cultured in RPMI 1640 (Gibco by Life Technologies) supplemented with 10% fetal bovine serum (Sigma-Aldrich), and maintained in a humidified atmosphere with 5% CO_2 at 37℃. Single cell suspension of ACs was cultured in ultra-low attachment plates (Corning) in the presence of serum-free DMEM/F12 (Wako) supplemented with 20 ng/mL EGF (Wako) and 10 ng/mL basic FGF (Wako), and maintained in a humidified atmosphere with 5% CO_2 at 37℃.

Inhibition of sphere formation

For the evaluation of the effect of metformin on sphere formation, suspension

of ACs was seeded at a density of 1×10^4 cells and cultured with 0.1 μM and 0.5 μM metformin for 24 hours under the same conditions as those for sphere formation. After 10 days of incubation, the number of spheres of > 50 μm size were counted.

Clonogenic cell survival assay

Cells were plated at various concentrations in 60 mm dishes and cultured for 24 hours with several concentrations of metformin. Cells were then X-ray irradiated and the medium was replaced with fresh growth medium. After incubation for 7 days, cells were fixed with methanol and stained with Giemsa's solution. Each colony consisting of more than 50 cells was scored as a colony forming unit. Survival fractions were calculated with a correction for plating efficiency of the cell death caused by metformin alone and dose-response curves were plotted. Three independent experiments were carried out, then the survival curves were fitted to a linear-quadratic model: $SF = (-\alpha D-\beta D^2)$, where SF is surviving fraction and D is the physical doses.

Intracellular ROS and superoxide analysis

Intracellular ROS and superoxide levels were evaluated using a commercial detection kit ROS-ID® (Enzo life Science, Farmingdale, NY, USA). SC and AC suspensions were prepared in normal culture flasks, and incubated for 24 hours, followed by the addition of 50 μM metformin at 24 hours prior to 5 Gy of X-ray irradiation. After irradiation, cells were trypsinized and resuspended in RPMI medium,

and at least 10^5 cells were analyzed by flow cytometry using FACS Callibur (BD Biosciences) according to the manufacturer's protocol. The mean fluorescence intensity of each sample was normalized to that of the ACs control. All data were analyzed using the CellQuest software package (BD Biosciences).

Measurement of oxygen consumption ratio (OCR) by electron spin resonance (ESR)

The ESR was performed as described previously with minor modification [Yamamoto *et al*., 2018]. The peak-to-peak line width of the ESR spectrum of lithium 5, 9, 14, 18, 23, 27, 32, 36-octa-n-butoxy-2, 3-naphthalocyanine (LiNc-BuO) shows a liner response to the partial pressure of oxygen (pO_2), and was used to measure oxygen consumption *in vitro*. The cells were suspended in 50 µl serum-free RPMI medium containing 0.1 mg LiNc-BuO and 2% dextran to avoid segmentation of the cells and LiNc-BuO particles after each treatment. Then, 30 µl of the cell suspension sample was immediately drawn into a glass capillary tube at the density of 7.5×10^4 per tube. ESR measurements were carried out using a JEOL-RE X-band spectrometer (JEOL, Tokyo, Japan) with a cylindrical TE011 mode cavity (JEOL). The cavity was maintained at 37℃ using a temperature controller (ES-DVT3; JEOL). The spectral line width was analyzed using a Win-Rad radical analyzer system (Radical Research, Tokyo, Japan). The line width of the ESR spectra versus pO_2 calibration curve was constructed from ESR measurements based on LiNc-BuO equilibrated with an oxygen/argon gas mixture.

Cellar ATP content analysis

Cellular ATP contents was evaluated using the ATP assay kit (Wako) according to the manufacture's protocol. SC and AC suspensions prepared in normal culture flasks were incubated for 24 hours with or without 50 µM metformin prior to 5 Gy of X-ray irradiation. After irradiation, the medium was replaced with fresh growth medium and cells were incubated for 24 hours, followed by cell trypsinization and resuspension in 100 µl serum-free RPMI medium at the density of 10^4 cells per well. Then, 100 µl of the ATP assay reagent was added, and chemiluminescence from each well was analyzed luminometer (Luminescencer-JNR; ATTO, Tokyo, Japan) set at 25℃.

Mitochondrial membrane potential analysis

The fluorescent probe tetramethyl rhodamine methyl ester (TMRM) was used for the analysis of mitochondrial membrane potential [Cottet-Rousselle *et al*., 2011]. SC and AC suspensions prepared in normal culture flasks were incubated for 24 hours followed by the addition of 50 µM of metformin at 24 hours prior to 5 Gy of X-ray irradiation. Cells were incubated with 50 nM TMRM for 30 minutes at 37℃, trypsinized and resuspended in RPMI, and at least 10^5 cells were analyzed by flow cytometry in similar way as described for ROS and superoxide evaluation.

Analysis of DNA kinetics by immunofluorescence staining for p53-binding protein 1 (53BP1)

The immunofluorescence staining for 53BP1 was performed as described previously in chapter I, with minor modification. ACs and SCs in exponential growth phase were seeded in a slide and cultured for 24 hours with or without metformin. At the indicated time after X-ray irradiation (1Gy), cells were fixed with 4% paraformaldehyde for 20 minutes at room temperature. Cells were permeabilized with PBS containing 0.5% Triton X-100 for 5 minutes at 4°C and blocked with PBS containing 6% goat serum for 30 minutes at RT. The blocked cells were incubated with a rabbit anti- 53BP1 antibody (Abcam) at 1:2,000 dilution in 3% goat serum overnight at 4°C and then incubated in the dark with an Alexa Fluor 488-conjugated anti-rabbit secondary antibody (Abcam) at a 1:2,000 dilution for 90 minutes. After incubation, they were counterstained with Prolong® Diamond Antifade Mountant with 4', 6'-diamidino-2-phenylindole (DAPI) (Thermo Fisher Scientific). Fluorescence microscopic analysis was performed using an Zeiss LSM 700 confocal laser microscope (Zeiss, St. Louis, MO, USA) with reflected light fluorescence, and foci were counted using Image J software (National Institutes of Health)

Analysis of signaling pathway by Western blotting

As previously described, ACs and SCs were collected and lysed with 1×SDS sample buffer (2% SDS, 10% glycerol, 6% β-mercaptoethanol, 50 mM Tris pH 6.8, and

0.001% bromophenol blue) after 24 hours exposure with 5 mM metformin or 5 Gy of X-irradiation or both. Then, sample was loaded on 5 and 10% w/v SDS-polyacrylamide gel, and transferred to the Whatman Protran nitrocellulose membrane (Merck, Tokyo, Japan) and the Immobilon^{TM}-P Transfer Membrane (Merck). Nonspecific antibody binding was blocked with 3% milk in PBS with Tween 20 for 30 minutes at RT with shaking. Membranes were incubated in primary antibody overnight on a shaker at 4˚C. Membranes were washed with a PBST buffer and then incubated in HRP-conjugated secondary antibody (Thermo Fisher Scientific, dilution 1:10,000 in PBST with 1% milk) for 1 hour on a shaker at RT. Membranes were washed as before and then incubated in HRP substrate for 5 minutes at RT. The protein antibody reaction were visualized with Western BLoT Ultra Sensitive HRP Substrate (TaKaRa Bio) and detected using an ImageQuant LAS-4000 mini system (GE Healthcare Japan, Tokyo, Japan). The following primary antibodies were used: polyclonal rabbit anti-phospho-AMPK α1 antibody (Thr172, #07-626) (Millipore, MD, USA), anti-AMPK α1 antibody (#07-350), anti-mTOR antibody (#2983) (Cell Signaling Technology Japan), anti-phospho-mTOR antibody (Ser2448, #5536), TSC2 antibody (#4308), anti- phospho-4EBP1antibody (Thy37/46, #2855), anti-phospho-70S6K antibody (Thr389, #9234), and β-actin (#4967). These antibodies were diluted 1:5,000 (TSC2) or 1:3,000 (the other antibodies) in PBST with 1% milk. These cross-reaction of these antibodies with canine molecules have been reported [Saeki *et al*., 2015].

Statistical analysis

For statistical analysis, JMP® 14 (SAS Institute Inc) software was used. All results are represented as the mean ± standard deviation (SD) values. Statistical analysis was performed using the Mann-Whitney's U test, and differences with p values of <0.05 were considered to be statistically significant.

RESULTS

Metformin inhibited sphere formation and sensitized SCs to radiation in vitro

ACs were cultured in serum free medium with EGF and bFGF. After 10 days of incubation without metformin, 63 ± 4 spheres with > 50 μm size were formed while 26 ± 3 and 3 ± 1 were formed when incubated with 10 and 50 μM metformin, respectively (FigureII-1A).

Exposure to metformin for 24 hours, reduced the clonogenic survival of SCs and ACs in a dose-dependent manner. In SCs, 10 and 50 μM metformin decreased the cell survival to 88.5% and 52.7%, respectively, while in ACs, the cells survival is 98.6% and 83.7%, respectively. The sensitivity of SCs to metformin was significantly higher compared to that of ACs (Figure II-1B). SCs and ACs were irradiated with 0, 2.5, 5.0, 7.5, and 10 Gy of X-ray with 10 μM and 50 μM metformin, and the colony formation was measured. The survival curve of SCs treated with metformin for 24 hours before irradiation was steeper than that of SCs treated with X-irradiation alone. In SCs, metformin showed significantly enhanced cell death induced by X-ray irradiation compared to control cells without metformin, whereas in ACs, there was no significant effect of metformin. (Figure II-1C).

Metformin, X-irradiation, and their combination induced intracellular ROS and superoxide production

Changes in the levels of intracellular ROS and superoxide by the treatment with metformin, X-irradiation, and metformin plus X-irradiation were evaluated. In ACs and SCs treated with metformin, X-irradiation, and metformin plus X-irradiation increased ROS and superoxide, as determined by the increase in the fluorescence intensity, compared to that in control, and the intensity in the treatment with metformin plus irradiation of SCs was far higher than metformin or irradiation alone (Figure II-2A). The difference in relative mean fluorescence intensity (MFI) between treatment (metformin, irradiation, and metformin plus irradiation) and control groups, was significantly higher in both ACs and SCs. However, ROS and superoxide levels of SCs treated with metformin, irradiation, and metformin plus irradiation, were significantly higher than those of ACs (Figure II-2B).

Metformin inhibited mitochondrial respiration, activated by X-irradiation

ROS and superoxide are considered as important parameters but activation and inhibition of mitochondrial respiration causes increment of ROS and superoxide production. Therefore, oxygen consumption was investigated to evaluate mitochondrial respiration. The pO_2 (mmHg) in the medium after each incubation time was calculated from the line width of the ESR spectrum by using the calibration curve. The oxygen consumption ratio (OCR) of ACs and SCs without any treatment (control) was calculated to be 5.21 ± 0.30 and 6.12 ± 0.31 mmHg/min/7.5×10^4 cells, respectively, by the linear relationship between pO_2 and time (Figure II-3A and B). Metformin inhibited

cellular oxygen consumption in ACs and SCs compared to control, 4.46 ± 0.09 and 3.58 ± 0.05 mmHg/min/7.5×10^4 cells, respectively. Irradiation, on the other hand, increased cellular oxygen consumption in ACs and SCs compared to control, 8.19 ± 0.49 and 14.67 ± 0.61 mmHg/min/7.5×10^4 cells, respectively. These changes in SCs were significantly higher than those in ACs. Additionally, X-irradiation induced oxygen consumption was decreased in SC treated with metformin plus irradiation, and OCR of SCs (3.19 ± 0.03) treated with metformin plus irradiation was significantly lower than that of control. However, OCR of ACs (5.58 ± 0.08) treated with metformin plus irradiation was comparable with control (Figure II-3C). According to these results, in SCs metformin inhibit irradiation-induced activation of mitochondrial respiration and decrease activated oxygen consumption as lower level than control.

Metformin inhibited ATP production induced by X-irradiation in SCs

Mitochondrial respiration is associated with cellular energy production. Metformin decreased ATP production, and irradiation increased ATP production in SCs. Moreover, ATP production of metformin plus irradiation significantly decreased than that of control. However, in ACs there was no significant difference in ATP production between control and treatment groups (metformin, irradiation, and metformin plus irradiation) (Figure II- 4). This data suggested that metformin and irradiation affect mitochondrial energy production in SCs.

X-irradiation increased mitochondrial membrane potential in SCs

The mitochondrial membrane potential, which indicates mitochondrial electron transport chain (ETC) activity, was investigated. Irradiation increased TMRM fluorescence intensity compared to respective control in ACs and SCs, whereas metformin decreased the intensity except for that in ACs with combined treatment (Figure II-5A). The difference in relative MFI between ACs and SCs was statistically significant in control, X-irradiation, and metformin plus X-irradiation (Figure II-5B). These results suggested that SCs had higher mitochondrial membrane potential under normal and irradiation conditions than ACs, and metformin decreased mitochondrial membrane potential especially in irradiated SCs.

SCs had a higher mitochondrial respiration capacity

To elucidate the difference in sensitivity to metformin and irradiation between ACs and SCs, the respiratory parameters were calculated as previously described using ESR oximetry by adding mitochondria-targeting reagents [Yamamoto *et al*., 2018]. The following four patterns of metabolic inhibitors were evaluated using ESR oximetry (1) without any reagents; (2) oligomycin A (an inhibitor of proton flow through ATP synthase, 1 μM); (3) oligomycin + CCCP (an ionophore that transports proton across the mitochondrial membrane leading to a collapse of the membrane potential and rapid consumption of O_2, 1 μM); (4) oligomycin + CCCP + combination of rotenone (an inhibitor of complex I, 1 μM) and antimycin A (an inhibitor of complex III, 1 μM) in

Figure II-6A. The respiratory parameters, including basal respiration, ATP-linked respiration, proton leak, maximal respiration, reserve capacity, and non-mitochondrial respiration, were calculated and summarized (Figure II-6B). Total mitochondrial ETC function of SCs, including basal respiration, ATP-linked respiration, proton leak, maximal respiration, and reserve capacity was significantly higher than that of ACs (Figure II-6C).

Metformin inhibited DNA double strand break repair of SCs following exposure to X-irradiation

To investigate whether metformin affects the kinetics of DNA double strand breaks (DSBs) rejoining, 53BP1 foci were measured after X-ray irradiation (1 Gy) in SCs and ACs with or without metformin. DSBs kinetics was different between ACs and SCs without metformin. The peak number of foci was significantly smaller and time-dependent reduction of foci was more rapid in SCs than in ACs. Additionally, metformin increased the peak number of foci and reduced time-dependent reduction of foci (Figure II-7). These results suggested that SCs possess enhanced DNA repair capacity and metformin inhibited the DNA repair especially in SCs.

Metformin did not affect activation of AMPK and its downstream effectors

To evaluate the effect of the AMPK/mTOR signaling pathway, the levels of protein expression and phosphorylation of AMPK, and its downstream targets mTOR,

S6K1 and 4EBP1, were measured in ACs and SCs treated with or without 50 μM of metformin at 24 hours after X-irradiation (5 Gy). In ACs and SCs, the levels of AMPK, p-AMPK, and its downstream targets mTOR, p-mTOR, p-S6K1 and p-4EBP1 were comparable with or without metformin, irradiation or metformin plus irradiation (Figure II-8A and B).

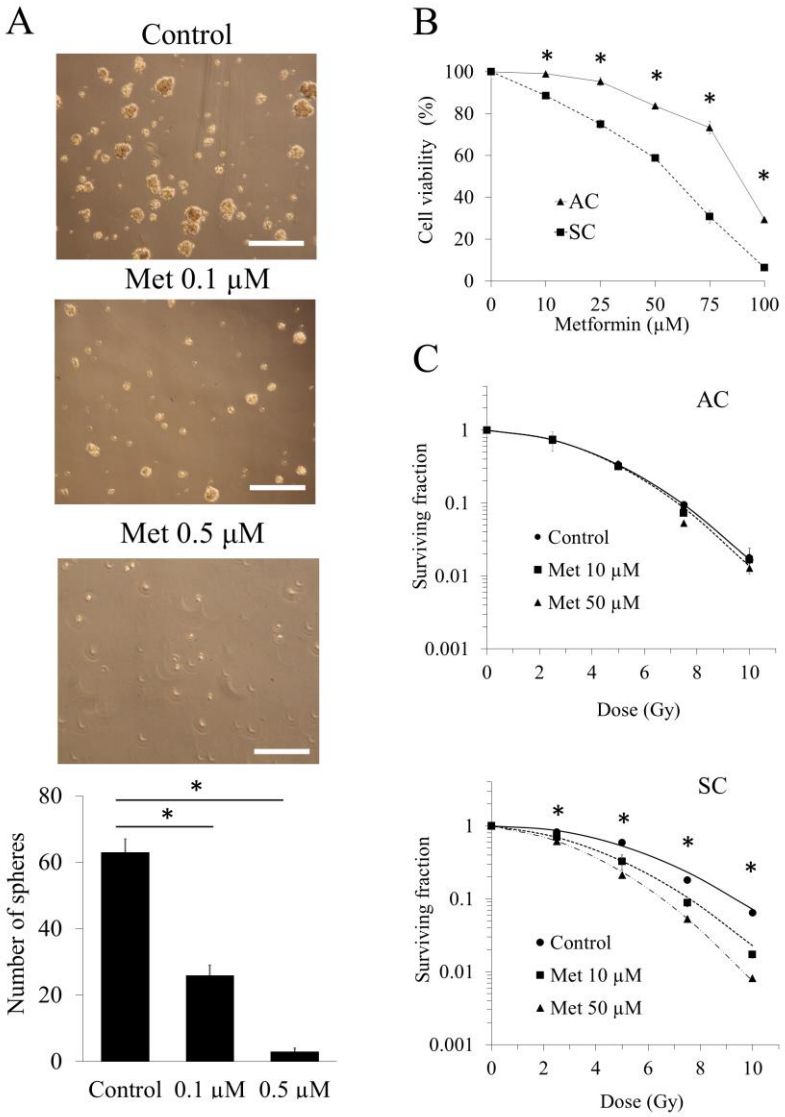

Figure II-1. Inhibition of sphere formation by metformin and survival curves of ACs and SCs treated radiation with or without metformin

Effects of metformin for sphere formation. Bar = 500 μm (A). Cell viability of treatment with 10-100 μM metformin for 24 hours in ACs and SCs (B). Survival curves of X-irradiation in ACs and SCs treated with or without metformin (C). These results were analyzed using Mann-Whitney *U* test. **p* < 0.05 for with versus without metformin.

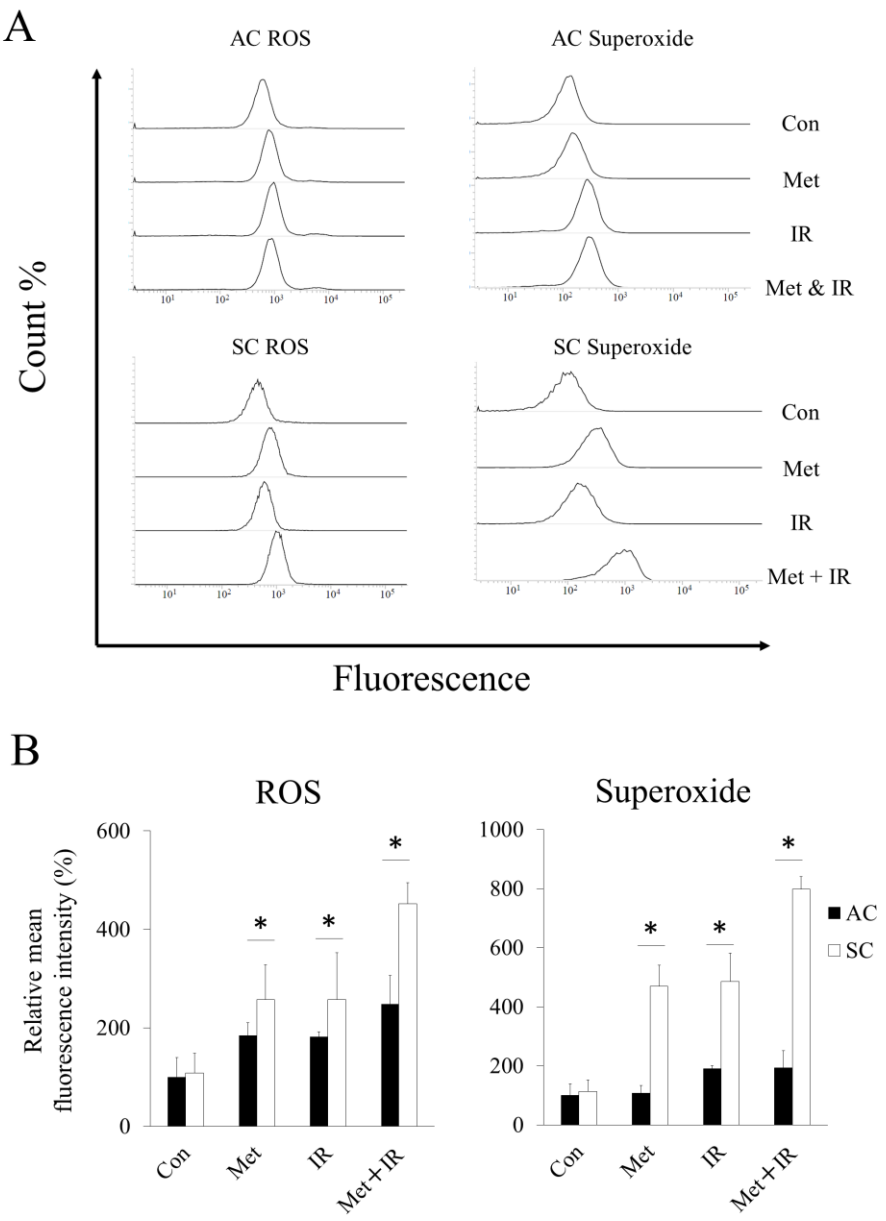

Figure II-2. Intracellular ROS and superoxide in ACs and SCs

Histogram of ACs and SCs of control (Con), 24 hours exposure with 50 μM metformin (Met), 5 Gy of X-irradiation (IR), and both metformin plus X-irradiation (Met + IR) (A). Relative mean fluorescence intensity (%) in ACs and SCs (B). These results were analyzed using Mann-Whitney *U* test. **p* < 0.05 for ACs versus SCs.

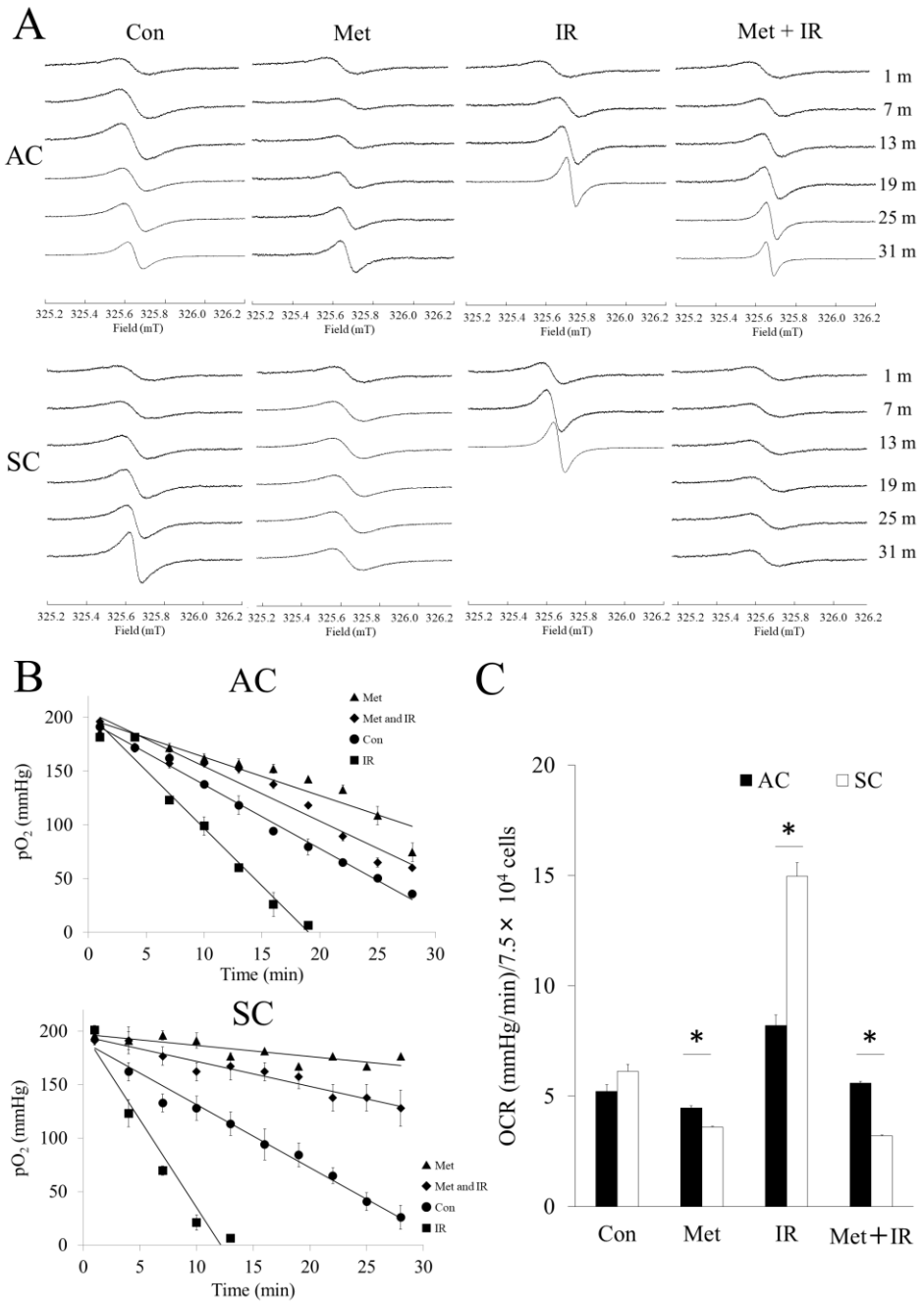

Figure II-3. ESR analysis of oxygen consumption in ACs and SCs.

Representative ESR spectra (A) and changes in pO_2 (B) of ACs and SCs treated with 50 μM metformin (Met), 5 Gy of X-irradiation (IR), and metformin plus X-irradiation (Met + IR). Oxygen consumption ratio (OCR) in ACs and SCs (C). These results were analyzed using Mann-Whitney *U* test. *$p < 0.05$ for ACs versus SCs.

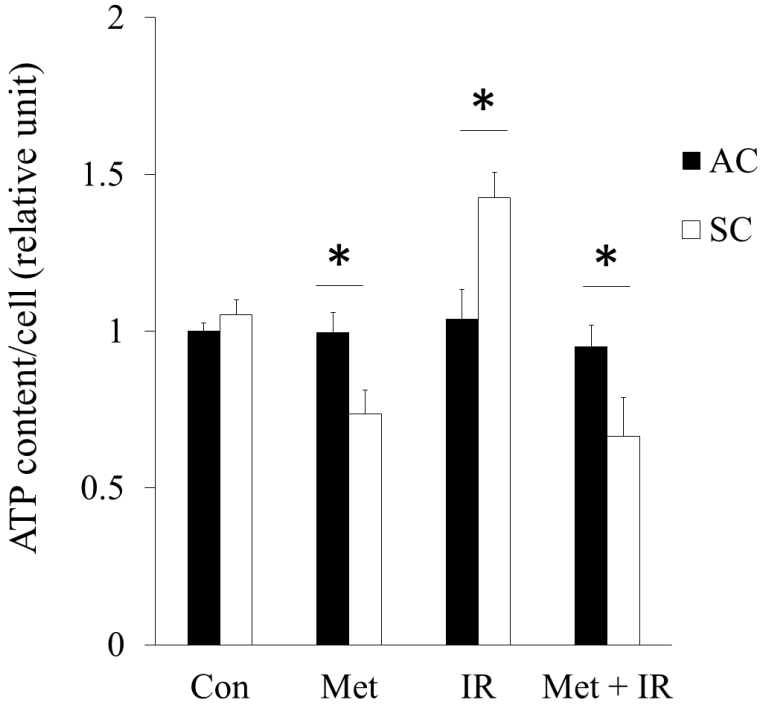

Figure II-4. Cellular ATP content in ACs and SCs

ATP contents of ACs and SCs treated with metformin (Met), X-irradiation (IR), and metformin plus X-irradiation (Met + IR). These results were analyzed using Mann-Whitney *U* test. *$p < 0.05$ for ACs versus SCs.

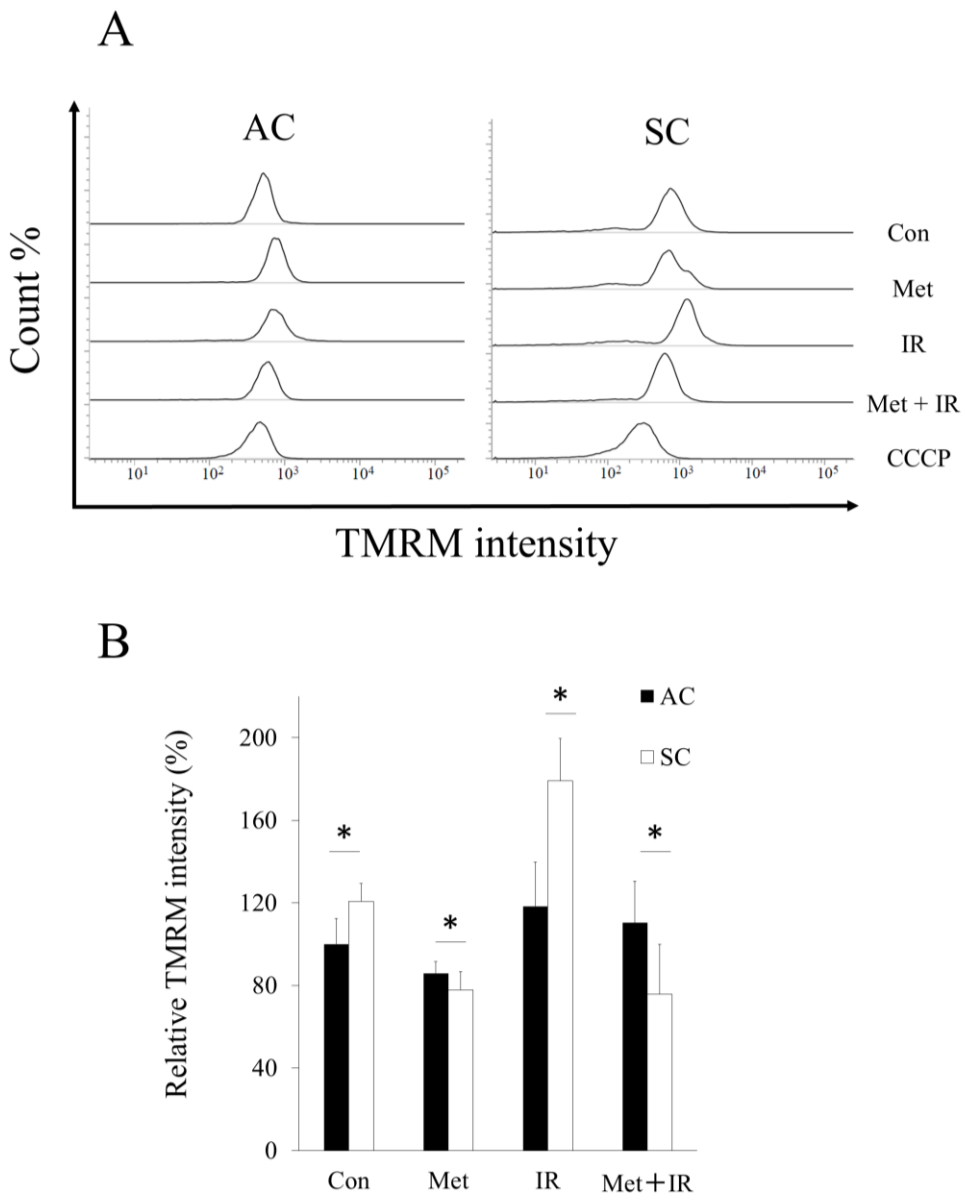

Figure II-5. Mitochondrial membrane potential in ACs and SCs.

Histogram of ACs and SCs of control (Con), 24 hours exposure with 50 μM metformin (Met), 5 Gy of X-irradiation (IR), and both metformin plus X-irradiation (Met + IR) (A). Relative TMEM intensity (%) in ACs and SCs. These results were analyzed using Mann-Whitney *U* test. *$p < 0.05$ for ACs versus SCs.

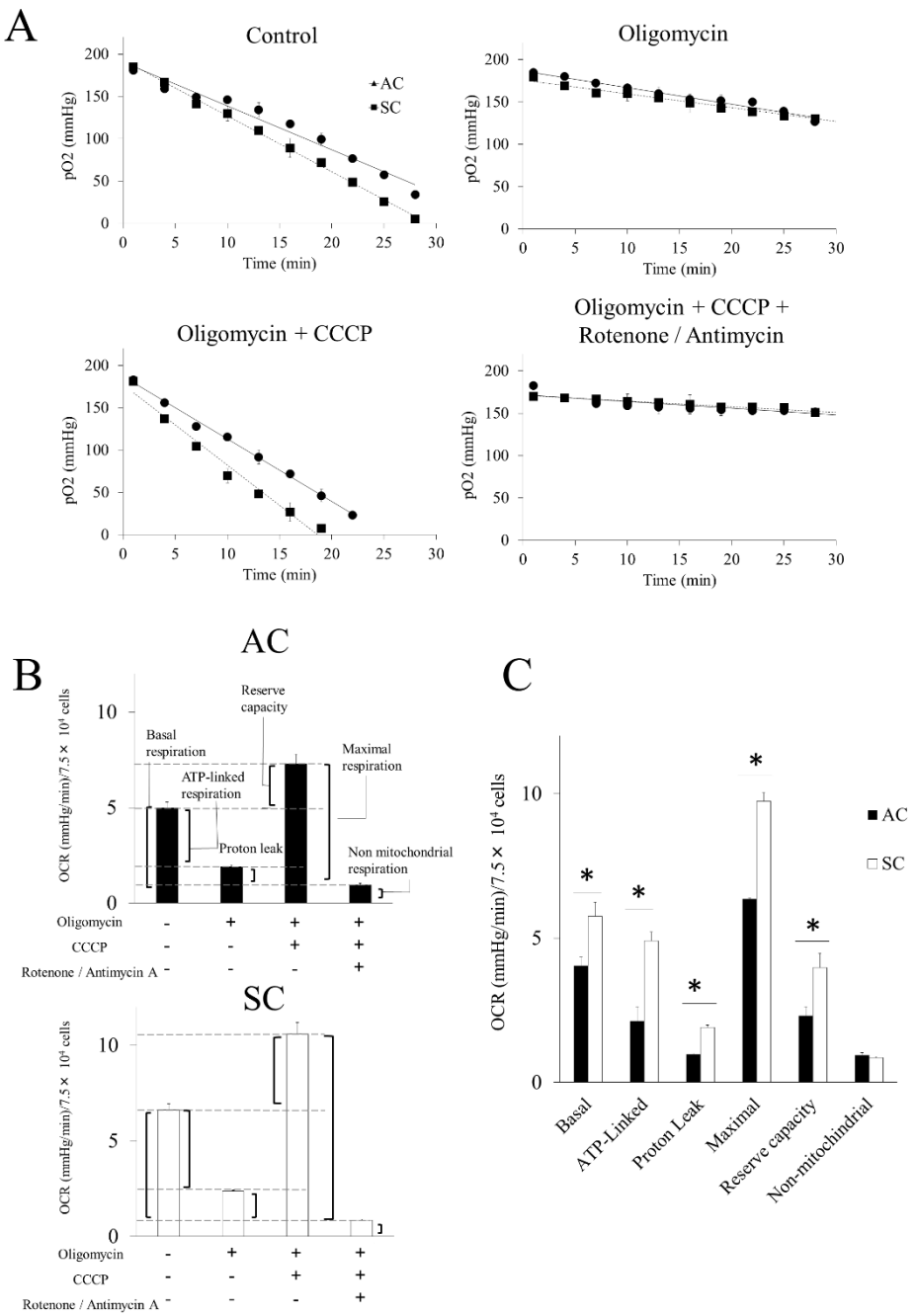

Figure II-6. Mitochondrial respiratory function of ACs and SCs.

Changes in pO_2 of ACs and SCs in the absence and the presence of mitochondria-targeting reagents (A). OCR in ACs and SCs in the absence and presence of a variety of mitochondria-targeting reagents (B and C). These results were analyzed using Mann-Whitney *U* test. *$p < 0.05$ for ACs versus SCs.

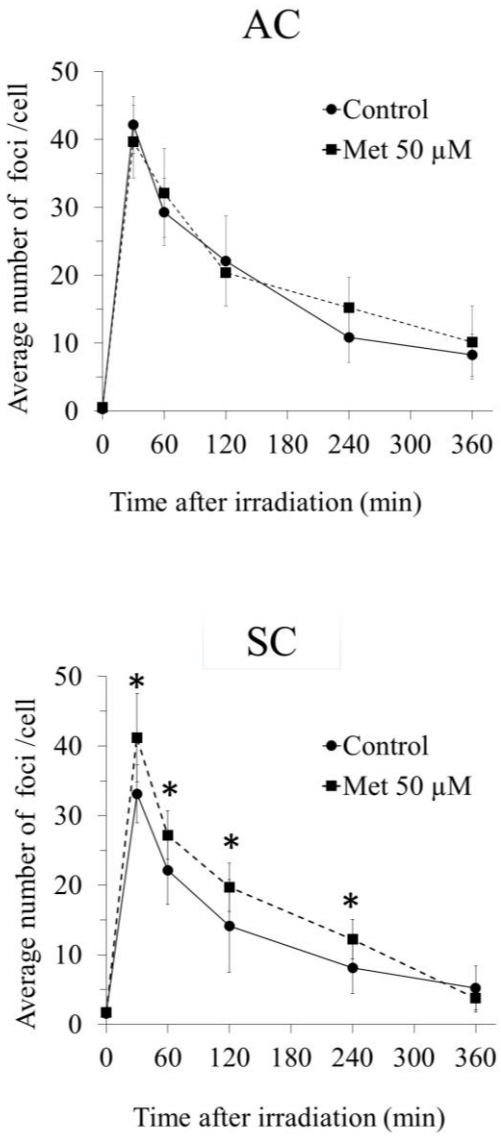

Figure II-7. DNA repair kinetics after X-ray irradiation with or without metformin in ACs and SCs.

Analysis of DNA repair kinetics for the formation of 53BP1 foci treated with or without metformin in ACs (■) and SCs (●) after 1 Gy of X-irradiation. These results were analyzed using Mann-Whitney *U* test. **p* < 0.05 for control versus metformin.

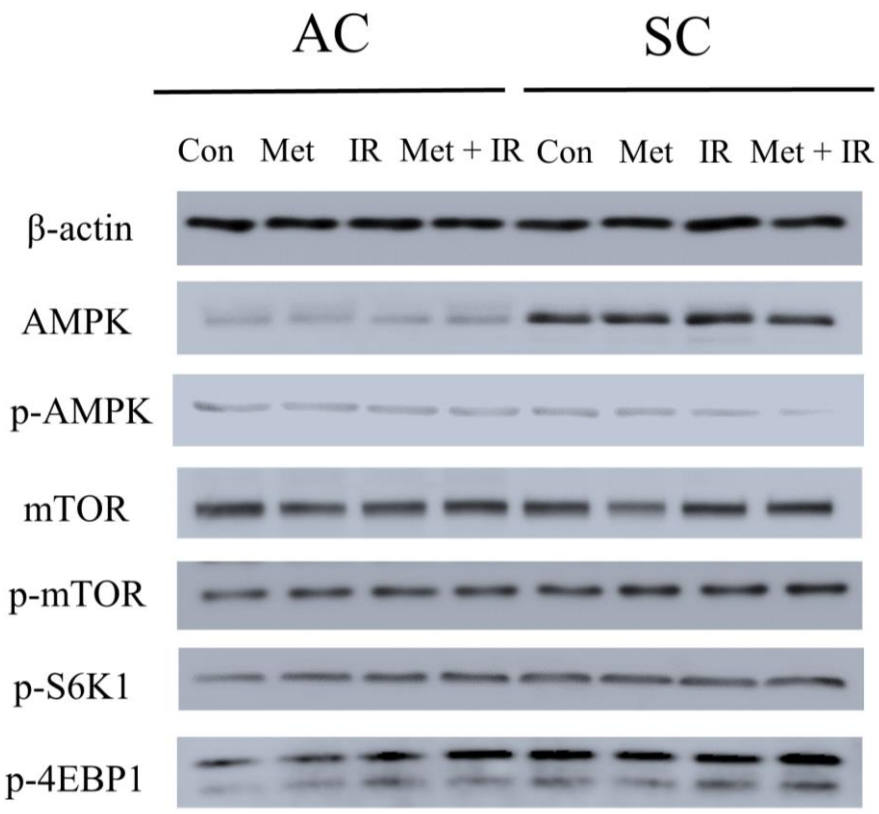

Figure II-8. Effect of metformin on phosphorylation of the AMPK/mTOR signaling pathway.

ACs and SCs were after 24 hours exposure with 50 μM metformin (Met) or 5 Gy of X-irradiation (IR) or both metformin plus X-irradiation (Met + IR).

DISCUSSION

Metformin is known to inhibit mitochondrial complex in the mitochondrial ETC chain, yet it is currently unknown whether the anti-cancer effect of metformin occurs through the inhibition of the mitochondrial complex. The present study evidence that metformin enhanced decrease in clonogenic cell survival of SCs after irradiation through the inhibition of mitochondrial respiration. Additionally, this effect of metformin was independent of AMPK phosphorylation. It was demonstrated that there were differences in mitochondrial respiration capacity between SCs and ACs. These differences in mitochondrial function might be linked to sensitivity to anti-cancer effect of metformin and irradiation.

Exposure to metformin for 24 hours at 50 μM concentration was preferentially cytotoxic and radio-sensitizing for SCs through inhibiting mitochondrial respiration and independently on AMPK activation. It has been reported that metformin killed CSCs through the activation of AMPK, which affects its downstream pathway (mainly mTOR signaling pathway), but these studies used 1-50 mM metformin and exposure time was over 24 hours [Song *et al*., 2012; Rocha *et al*., 2018]. Exposure to lower concentration of metformin, 5-25 μM, for 1-72 hours enhanced radiation-induced cell death, whereas AMPK activation reached high levels after 48-72 hours of metformin exposure [Fasih *et al*., 2014]. According to these results, AMPK activation by metformin is a secondary phenomenon that occurred after the decrease in ATP production by mitochondrial

respiration [Owen *et al*., 2000; Rena *et al*., 2017], and low concentration and short exposure time of metformin can radio-sensitize cancer cells through inhibiting the mitochondrial respiration, but not through AMPK activation.

It was demonstrated that metformin induces a lethal energy crisis by enhancing ROS production, and reducing ATP levels and mitochondrial membrane potential in SCs. Furthermore, it was also found that metformin inhibits cellular oxygen consumption as an indicator of metformin toxicity at the cellular level in SCs. Increment of intracellular ROS levels are involved in DNA damage, disturbing cell redox balance, and signal transduction pathways [Biswas *et al*., 2006]. It has been suggested that metformin increases intracellular ROS level, thus providing an alternative mechanism to AMPK activation [Hou *et al*., 2018]. Metformin also decreased mitochondrial respiration, membrane potential, and ATP production, suggesting it caused suppression of ETC function. Recent researches have demonstrated a role for the inhibition of mitochondrial complex in the anticancer effect of metformin [Wheaton *et al*., 2014; Birsoy *et al*., 2014]. The improving mitochondrial-targeting metformin analogues are much more potent than metformin in inhibiting cancer cells [Kalyanaraman *et al*., 2017]. These results suggested that the anti–cancer effect of metformin depends on the inhibition of the mitochondrial complex and disturbing metabolism of mitochondria.

To elucidate the difference in metformin sensitivity between ACs and SCs, the mitochondrial function was compared using ESR oximetry [Yamamoto *et al*., 2018]. In

this study, SCs had higher mitochondrial function than ACs under both non-irradiation and irradiation condition, which were indicated by high ability of mitochondrial basal, ATP-linked, maximal respiration, and proton leak in SCs. This result suggested SCs had a high level of oxidative phosphorylation. It is known that cancer cells preferentially use anaerobic glycolysis compared to normal tissues, that is referred to as Warburg effect, but metabolic features of CSCs have still remained controversial [Zhou *et al*., 2011]. Several reports have shown that CSCs rely more on oxidative phosphorylation than on glycolysis for their energy supply [Folmes *et al*., 2011; Sun *et al*., 2017]. This observation can explain why metformin is more effective for CSC because metformin is more effective in cells with high cellular oxidative phosphorylation, which correlates with high ability of mitochondrial respiration.

To our knowledge, it has reported for the first time that SCs have high ability for mitochondrial respiration and can activate their respiration when irradiated, which induces intracellular ROS and ATP production, and increase mitochondrial membrane potential. Irradiation increases oxidative phosphorylation of cells, which have high mitochondrial reserve capacity [Yamamori *et al*., 2012]. Reserve capacity indicates ability of cells to increase oxidative phosphorylation in order to respond to stress such as irradiation [Gao *et al*., 2016]. It is still unknown whether the activation of mitochondrial metabolism contributes to cell fate decisions, but several reports demonstrated that mitochondrial ATP production enhanced cell survival after irradiation [Azzam *et al*., 2012]. Furthermore, SCs had a high DNA repair capacity and metformin

inhibited DNA repair in SCs. These results showed that mitochondrial function and ATP production were linked with radio-resistance of cancer cells. For example, ATP-dependent chromatin remodeling complexes in DSB repair and PARP activity are ATP dependent [Goetze *et al*., 2013; Lynam-Lennon *et al*., 2014; Pawlik and Keyomarsi, 2004]. Thus, mitochondrial function might play an important role in cells' radio-sensitivity, and high mitochondrial respiratory capacity of CSCs might be linked to their radio-resistance through DNA repair.

In summary, metformin preferentially radiosensitized SCs, through inhibiting mitochondrial respiration. Additionally, SCs had a higher ability of mitochondrial respiration than ACs, which might account for the differences in their radio-sensitivity. Therefore, mitochondrial function might play an important role in the radio-resistance mechanism in CSCs and drugs targeting mitochondrial respiration, such as metformin could be a promising radio-sensitizer in CSC.

SUMMARY

Metformin has been reported to have many anti-cancer effect, alone or in combination with ionizing radiation. However, the mechanism underlying its radio-sensitizing effect is still unclear, especially for cancer stem-like cells (CSCs). Here, the radio-sensitizing effect of metformin was investigated and its mechanism was revealed in CSCs derived from HMPOS, a canine osteosarcoma cell line. Spheroid cells (SCs) were used as a CSCs-rich cells derived from sphere formation and SCs were compared with normal adherent culture cells (ACs). The radio-sensitizing effect of metformin using clonogenic assay was evaluated and the mechanism of its radio-sensitization focusing on mitochondrial function was revealed. Metformin significantly enhanced radiosensitivity of SCs through its inhibition of the mitochondrial function, as shown by the induction of intracellular ROS, decreased oxygen consumption, and decreased mitochondrial membrane potential. Additionally, SCs had a higher ability of mitochondrial respiration than ACs, which may have caused difference of their sensitivity of metformin and radiation. In conclusion, mitochondrial function might play an important role in the sensitivity of metformin and irradiation in CSCs and drugs that targeting mitochondrial respiration such as metformin are promising radio-sensitizer to target CSCs.

CONCLUSION

The aim of this study is to elucidate the existence of CSCs as a cause of the resistance to radiation therapy of dog tumor, and to analyze their characteristic, which can contribute to establish novel strategy for targeting CSCs and improving patient outcome. CSCs derived from canine tumor cell lines were investigated to determine whether they possess the same characteristics of human CSCs, and whether they show lower radiosensitivity than their corresponding parent cells. Then, to search drugs effective for CSCs and elucidate the mechanism of radiation resistance of CSCs, the effect and mechanism of metformin as a radio-sensitizer were evaluated in CSCs.

In chapter I, to isolate CSCs from canine cancer cell lines and to elucidate relation between canine CSCs and radio-sensitivity of tumor, spheroid cells (SCs) were isolated from four canine tumor cell lines (osteosarcoma, melanoma, traditional cell carcinoma, and lung adenocarcinoma) by the culture using sphere formation and evaluated if they have CSCs-like properties, including expression of CSCs makers, tumorigenic capacity, and radio-sensitivity. All SCs isolated using sphere formation showed high *CD133* expression and tumorigenic ability compared to parental adherent cells (ACs) in normal culture condition. All SCs were significantly resistant against X-irradiation compared to ACs. In addition, the amount of DNA double strand breaks after X-irradiation was significantly lower in SC than in the corresponding AC. These results showed that SCs isolated via sphere formation possess CSCs-like characteristics and

CSCs are important factor that affect radiosensitivity in canine tumors.

In chapter II, to establish therapeutic strategy targeting CSCs, the radio-sensitizing effect of metformin and its mechanism of anti-cancer effect were investigated. It has been reported metformin has many anti-cancer effect, alone or in the combination with ionizing radiation. However, the mechanism underlying its radio-sensitized effect is still unclear, especially for CSCs. SCs was isolated from a canine osteosarcoma cell line by sphere formation culture of original ACs, and used as radio-resistance CSCs model. The radio-sensitizing effect of metformin was examined by using clonogenic assay, and it was revealed the mechanism of its radio-sensitization focusing on mitochondrial function. Metformin preferentially radio-sensitized SCs leading to inhibiting mitochondrial respiration, as determined by the induction of intracellular ROS, decrease of oxygen consumption, ATP, and mitochondrial membrane potential. Additionally, to elucidate high sensitivity of radio-sensitizing effect of metformin to SCs as compared with ACs, the respiratory ability of mitochondria was evaluated and SCs had a higher ability of mitochondrial respiration than ACs. According to these results, mitochondrial respiration might play a central role in the radio-resistance mechanism of CSCs and metformin is a promising radio-sensitizer that can inhibit mitochondrial respiration of CSCs.

Taken together, CSCs were shown to be important as a factor determining radiosensitivity in canine tumors. In addition, metformin targeting mitochondria of radio-resistant CSCs was shown to be effective as a radio-sensitizer, and the possibility

that high ability of mitochondrial respiration may be involved in radio-resistance of CSCs has been shown.

ACKNOWLEDGEMENT

I would like to express my deepest gratitude to my professors, Dr. Masahiro Okumura, Dr. Kenji Hosoya, and Dr. Shango Kim, in Laboratory of Veterinary Surgery, Department of Clinical Sciences, Graduate school of Veterinary Medicine, Hokkaido University (Sapporo, Japan), for their continuous mentoring, guidance, assistance, and encouragement through the course of this study.

I greatly appreciate, Dr. Osamu Inanami, Dr. Hironobu Yasui, Dr. Tohru Yamamori, and all members in Laboratory of Radiation Biology, Department of Applied Veterinary Sciences, Graduate school of Veterinary Medicine, Hokkaido University, on their pivotal help in radiation biology research, technical advice, and assistance on the research.

I would like to express my sincere appreciation to Dr. Kazuhiko Ohashi, in Laboratory of Infectious Diseases, Department of Disease Control, Faculty of Veterinary Medicine, Hokkaido University, for their invaluable advice on the experiments and critical review on the manuscript.

I am deeply grateful to Dr. Keisuke Aoshima, in Laboratory of Comparative Pathology, Department of Clinical Medicine, Faculty of Veterinary Medicine Hokkaido University, for his technical assistance in histopathology.

I owe a deep debt of gratitude to Dr. Naoya Maekawa, in Laboratory of Infectious Diseases, Department of Disease Control, Faculty of Veterinary Medicine,

Hokkaido University, for his technical assistance.

I greatly thank to Dr. Hiroki Sahara, Laboratory of Biology, School of Veterinary Medicine, Azabu University (Sagamihara, Japan), Dr. Takayuki Nakagawa, Laboratory of Veterinary Surgery, Graduate school of Agricultural and Life Science, The University of Tokyo (Tokyo, Japan), and Dr. Yuki Hoshino, Department of Small Animal Surgery, Faculty of Agriculture, Iwate University (Morioka, Japan) for providing canine cancer cell lines, CLAC, CMeC and MegTCC, respectively.

I would like to extend my sincere condolences on the death of experimental animals that were used for my research.

Special deep thanks are extended to all members in Laboratory of Veterinary Surgery and Veterinary Teaching Hospital, Faculty of Veterinary Medicine, Hokkaido University, for their excellent help and warm friendship.

I would like to show my deep appreciation to my family and friends for their encouragement and support throughout the course of my education and research.

Finally, I would like to thank all people who helped me to complete this study. Thank you so much.

REFERENCES

Azzam, E. I., Jay-Gerin, J. P., and Pain, D. Ionizing radiation-induced metabolic oxidative stress and prolonged cell injury. *Cancer Lett.*; 2012, **327**, 48-60.

Bao, S. D., Wu, Q. L., McLendon, R. E., Hao, Y. L., Shi, Q., Hjelmeland, A. B., Dewhirst, M. W., Bigner, D. D., and Rich, J. N. Glioma stem cells promote radioresistance by preferential activation of the DNA damage response. *Nature*; 2006, **444**, 756-760.

Barroga, E. F., Kadosawa, T., Okumura, M., and Fujinaga, T. Establishment and characterization of the growth and pulmonary metastasis of a highly lung metastasizing cell line from canine osteosarcoma in nude mice. *J. Vet. Med. Sci.*; 1999, **61**, 361-367.

Baumann, M. and Krause, M. CD44: A cancer stem cell-related biomarker with Predictive Potential for Radiotherapy. *Clin. Cancer. Res*; 2006, **16**, 5091-5093.

Bertolini, G., Roz, L., Perego, P., Tortoreto, M., Fontanella, E., Gatti, L., Pratesi, G., Fabbri A., Andriani, F., Tinelli, S., Roz, E., Caserini, R., Lo Vullo, S., Camerini, T., Mariani, L., Delia, D., Calabro, E., Pastorino, U., and Sozzi, G. Highly tumorigenic lung cancer CD133 (+) cells display stem-like features and are spared by

cisplatin treatment. *Proc. Nati. Acad. Sci. USA*; 2009, **106**, 16281-16286.

Birsoy, K., Possemato, R., Lorbeer, F. K., Bayraktar, E. C., Thiru, P., Yucel, B., Wang, T., Chen, W. W., Clish, C.B., and Sabatini, D. M. Metabolic determinants of cancer cell sensitivity to glucose limitation and biguanides. *Nature*; 2014, **508**, 108.

Biswas, S., Chida, A. S., and Rahman, I. Redox modifications of protein-thiols: Emerging roles in cell signaling. *Biochem. Pharmacol.*; 2006, **71**, 551-564.

Bonnet, D. and Dick, J. E. Human acute myeloid leukemia is organized as a hierarchy that originates from a primitive hematopoietic cell. *Nat. Med.*; 1997, **3**, 730-737.

Bortfeld, T. and Schlegel, W. Optimization of beam orientations in radiation therapy some theoretical considerations. *Phys. Med. Bio.*; 1993, **38**, 291-304.

Brenner, D. J. and Hall, E. J. Fractionation and protraction for radiotherapy of prostate carcinoma. *Int. J. Radiat. Oncol. Biol. Phys.*; 1999, **43**, 1095-1101.

Cao, L., Zhou, Y. M., Zhai, B. B., Liao, J., Xu, W., Zhang, R. X., Li, J., Zhang, Y., Chen, L., Qian, H. H., Wu, M. C., and Yin, Z. M. Sphere-forming cell subpopulations with cancer stem cell properties in human hepatoma cell lines. *BMC Gastroenterol.*;

2011, **11**, 71.

Chang, C. H., Zhang, M., Rajapakshe, K., Coarfa, C., Edwards, D., Huang, S. X., and Rosen, J. M. Mammary stem cells and tumor-initiating cells are more resistant to apoptosis and exhibit increased DNA repair activity in response to DNA damage. *Stem Cell Reports*; 2015, **5**, 378-391.

Chen, Y. C., Hsu, H. S., Chen, Y. W., Tsai, T. H., How, C. K., Wang, C. Y., Hung, S. C., Chang, Y. L., Tsai, M. L., Lee, Y. Y., Ku, H. H., and Chiou, S. H. Oct-4 expression maintained cancer stem-like properties in lung cancer-derived CD133-positive cells. *PLoS One*; 2008, **3**, 7.

Chun, S. G., Hu, C., Choy, H., Komaki, R. U., Timmerman, R. D., Schild, S. E., Bogart, J. A., Dobelbower, M. C., Bosch, W., Galvin, J. M., Kavadi, V. S., Narayan, S., Iyengar, P., Robinson, C. G., Wynn, R. B., Raben, A., Augspurger, M. E., MacRae, R., Paulus, R., and Bradley, J. D. Impact of intensity-modulated radiation therapy technique for locally advanced non-small-cell lung cancer: A secondary analysis of the NRG Oncology RTOG 0617 randomized clinical trial. *J. Clin. Oncol.*; 2017, **35**, 56.

Collins, A. T., Berry, P. A., Hyde, C., Stower, M. J., and Maitland, N. J. Prospective

identification of tumorigenic prostate cancer stem cells. *Cancer Res.*; 2005, **65**, 10946-10951.

Coomer, A., Farese, J., Milner, R., Liptak, J., Bacon, N., and Lurie, D. Radiation therapy for canine appendicular osteosarcoma. *Vet. Comp. Oncol.*; 2009, **7**, 15-27.

Cottet-Rousselle, C., Ronot, X., Leverve, X., and Mayol, J. F. Cytometric assessment of mitochondria using fluorescent probes. *Cytometry A*; 2011, **79**, 405-425.

Dolera, M., Malfassi, L., Marcarini, S., Mazza, G., Carrara, N., Pavesi, S., Sala, M., Finesso, S., and Urso, G. High dose hypofractionated frameless volumetric modulated arc radiotherapy is a feasible method for treating canine trigeminal nerve sheath tumors. *Vet. Radiol. Ultrasound.*; 2018, **59**, 624-631.

Eramo, A., Lotti, F., Sette, G., Pilozzi, E., Biffoni, M., Di Virgilio, A., Conticello, C., Ruco, L., Peschle, C., and De Maria, R. Identification and expansion of the tumorigenic lung cancer stem cell population. *Cell Death Differ.*; 2008, **15**, 504-514.

Fargeas, C. A., Florek, M., Huttner, W. D., and Corbeil, D. Characterization of prominin-2, a new member of the prominin family of pentaspan membrane glycoproteins. *J. Biol. Chem.*; 2003, **278**, 8586-8596.

F**asih, A., Elbaz, H. A., Huttemann, M., Konski, A.A., and Zielske, S. P.** Radiosensitization of pancreatic cancer cells by metformin through the AMPK pathway. *Radiat. Res.*; 2014, **182**, 50-59.

Finley, L. W. S., Carracedo, A., Lee, J., Souza, A., Egia, A., Zhang, J. W., Teruya-Feldstein, J., Moreira, P. I., Cardoso, S. M., Clish, C. B., Pandolfi, P. P., and Haigis, M. C. SIRT3 opposes reprogramming of cancer cell metabolism through HIF1 alpha destabilization. *Cancer Cell*; 2011, **19**, 416-428.

Folmes, C. D. L., Nelson, T. J., Martinez-Fernandez, A., Arrell, D. K., Lindor, J. K., Dzeja, P. P., Ikeda, Y., Perez-Terzic, C., and Terzic, A. Somatic oxidative bioenergetics transitions into pluripotency-dependent glycolysis to facilitate nuclear reprogramming. *Cell Metab.*; 2011, **14**, 264-271.

Frisch, S. M. and Francis, H. Disruption of epithelial cell-matrix interactions induces apoptosis. *J. Cell. Biol.*; 1998, **124**, 619-626.

Gao, C. C., Shen, Y., Jin, F., Miao, Y. J., and Qiu, X. F. Cancer stem cells in small cell lung cancer cell line H446: Higher dependency on oxidative phosphorylation and mitochondrial substrate-level phosphorylation than non-stem cancer cells. *PLoS One*; 2016, **11**, 5.

Goetze, K., Yaromina, A., Zips, D., Baumann, M., and Mueller, W. Glycolysis-related gene induction and ATP reduction during fractionated irradiation. Markers for radiation responsiveness of human tumor xenografts. *Strahlenther Onkol.*; 2013, **189**, 782-788.

Goodell, M. A., Brose,K., Paradis, G., Conner, A. S., and Mulligan, R. C. Isolation and functional properties of murine hematopoietic stem cells that are replicating *in vivo*. *J. Exp. Med.*; 1996, **183**, 1797-1806.

Guth, A. M., Deogracias, M., and Dow, S. W. Comparison of cancer stem cell antigen expression by tumor cell lines and by tumor biopsies from dogs with melanoma and osteosarcoma. *Vet. Immunol. Immunopathol.*; 2014, **161**, 132-140.

Han, Z. and Papermaster, D. S. Identification of three prominin homologs and characterization of their messenger RNA expression in Xenopus laevis tissues. *Mol. Vis.*; 2011, **17**, 1381-1396.

Haraguchi, N., Utsunomiya, T., Inoue, H., Tanaka, F., Mimori, K., Barnard, G. F., and Mori, M. Characterization of a side population of cancer cells from human gastrointestinal system. *Stem Cells*; 2006, **24**, 506-513.

Ho, M. M., Ng, A. V., Lam, S., and Hung, J. Y. Side population in human lung cancer cell lines and tumors is enriched with stem-like cancer cells. *Cancer Res.*; 2007, **67**, 4827-4833.

Hou, W. L., Yin, J., Alimujiang, M., Yu, X. Y., Ai, L. G., Bao, Y. Q., Liu, F., and Jia, W. P. Inhibition of mitochondrial complex I improves glucose metabolism independently of AMPK activation. *J. Cell. Mol. Med.*; 2018, **22**, 1316-1328.

Inoue, K., Ohashi, E., Kadosawa, T., Hong, S. H., Matsunaga, S., Mochizuki, M., Nishimura, R., and Sasaki, N. Establishment and characterization of four canine melanoma cell lines. *J. Vet. Med. Sci.*; 2004, **66**, 1437-1440.

Isayev, O., Rausch, V., Bauer, N., Liu, L., Fan, P., Zhang, Y. Y., Gladkich, J., Nwaeburu, C. C., Mattern, J., Mollenhauer, M., Ruckert, F., Zach, S., Haberkorn, U., Gross, W., Schonsiegel, F., Bazhin A. V., and Herr, I. Inhibition of glucose turnover by 3-bromopyruvate counteracts pancreatic cancer stem cell features and sensitizes cells to gemcitabine. *Oncotarget.*; 2014, **5**, 5177-5189.

Ishimoto, T., Nagano, O., Yae, T., Tamada, M., Motohara, T., Oshima, H., Oshima, M., Ikeda, T., Asaba, R., Yagi, H., Masuko, T., Shimizu, T., Ishikawa, T., Kai, K., Takahashi, E., Imamura, Y., Baba, Y., Ohmura, M., Suematsu, M., Baba, H., and

Saya, H. CD44 variant regulates redox status in cancer cells by stabilizing the xCT subunit of system xc (-) and thereby promotes tumor growth. *Cancer Cell*; 2011, **19**, 387-400.

Jaszai, J., Fargeas, C. A., Graupner, S., Tanaka, E. M., Brand, M., Huttner, W. B., and Corbeil, D. Distinct and conserved prominin-1/CD133-positive retinal cell populations identified across species. *PLoS One*; 2011, **6**, 3.

Kalyanaraman, B., Cheng, G., Hardy, M., Ouari, O., Sikora, A., Zielonka, J., and Dwinell, M. B. Modified metformin as a more potent anticancer drug: Mitochondrial inhibition, redox signaling, antiproliferative effects and future EPR studies. *Cell Biochem. Biophys.*; 2017, **75**, 311-317.

Kondo, T., Setoguchi, T., and Taga, T. Persistence of a small subpopulation of cancer stem-like cells in the C6 glioma cell line. *Proc. Nati. Acad. Sci. USA*; 2004, **101**, 781-786.

Koppenol, W. H., Bounds, P. L., and Dang, C. V. Otto Warburg's contributions to current concepts of cancer metabolism. *Nat. Rev. Cancer*; 2011, **11**, 325-337.

Ling, C. C., Burman, C., Chui, C. S., Kutcher, G. J., Leibel, S. A., LoSasso, T., Mohan, R., Bortfeld, T., Reinstein, L., Spirou, S., Wang, X. H., Wu, Q. W.,

Zelefsky, M., and Fuks, Z. Conformal radiation treatment of prostate cancer using inversely-planned intensity-modulated photon beams produced with dynamic multileaf collimation. *Int. J. Radiat. Oncol. Biol. Phys.*; 1998, **35**, 721-730.

Lonardo, E., Cioffi, M., Sancho, P., Sanchez-Ripoll, Y., Trabulo, S. M., Dorado, J., Balic, A., Hidalgo, M., and Heeschen, C. Metformin targets the metabolic achilles heel of human pancreatic cancer stem cells. *PLoS One*; 2013, **8**, 10.

Lukas, J., Lukas, C., and Bartek, J. More than just a focus: The chromatin response to DNA damage and its role in genome integrity maintenance. *Nat. Cell. Biol.*; 2011, **13**, 1161-1169.

Lynam-Lennon, N., Maher, S. G., Maguire, A., Phelan, J., Muldoon, C., Reynolds, J. V., and O'Sullivan, J. Altered mitochondrial function and energy metabolism is associated with a radioresistant phenotype in oesophageal adenocarcinoma. *PLoS One*; 2014, **9**, 6.

Marcato, P., Dean, C. A., Giacomantonio, C. A., and Lee, P. W. K. Aldehyde dehydrogenase: Its role as a cancer stem cell marker comes down to the specific isoform. *Cell Cycle*; 2011, **10**, 1378-1384.

Martin, O. A., Ivashkevich, A., Choo, S., Woodbine, L., Jeggo, P. A., Martin, R. F., and Lobachevsky, P. Statistical analysis of kinetics, distribution and co-localisation of DNA repair foci in irradiated cells: Cell cycle effect and implications for prediction of radiosensitivity. *DNA Repair*; 2013, **12**, 844-855.

Martins-Neves, S. R., Lopes, A. O., Carmo, A., Paiva, A. A., Simoes, P. C., Abrunhosa, A. J., and Gomes, C. M. T. Therapeutic implications of an enriched cancer stem-like cell population in a human osteosarcoma cell line. *BMC Cancer*; 2012, **12**, 139.

Michishita, M., Akiyoshi, R., Suemizu, H., Nakagawa, T., Sasaki, N., Takemitsu, H., Arai, T., and Takahashi, K. Aldehyde dehydrogenase activity in cancer stem cells from canine mammary carcinoma cell lines. *Vet. J.*; 2012, **193**, 508-513.

Michishita, M., Akiyoshi, R., Yoshimura, H., Katsumoto, T., Ichikawa, H., Ohkusu-Tsukada, K., Nakagawa, T., Sasaki, N., and Takahashi, K. Characterization of spheres derived from canine mammary gland adenocarcinoma cell lines. *Res. Vet. Sci.*; 2011, **91**, 254-260.

Mizugaki, H., Sakakibara-Konishi, J., Kikuchi, J., Moriya, J., Hatanaka, K. C., Kikuchi, E., Kinoshita, I., Oizumi, S., Dosaka-Akita, H., Matsuno, Y., and

Nishimura, M. CD133 expression: A potential prognostic marker for non-small cell lung cancers. *Int. J. Clin. Oncol.*; 2014, **19**, 254-259.

Murase, M., Kano, M., Tsukahara, T., Takahashi, A., Torigoe, T., Kawaguchi, S., Kimura, S., Wada, T., Uchihashi, Y., Kondo, T., Yamashita, T., and Sato, N. Side population cells have the characteristics of cancer stem-like cells/cancer-initiating cells in bone sarcomas. *Br. J. Cancer*; 2009, **101**, 1425-1432.

Nemoto, Y., Maruo, T., Sato, T., Deguchi, T., Ito, T., Sugiyama, H., Ishikawa, T., Madarame, H., Watanabe, T., Shida, T., and Sahara, H. Identification of cancer stem cells derived from a canine lung adenocarcinoma cell line. *Vet. Pathol.*; 2011, **48**, 1029-1034.

Owen, M. R., Doran, E., and Halestrap, A. P. Evidence that metformin exerts its anti-diabetic effects through inhibition of complex 1 of the mitochondrial respiratory chain. *Biochem. J.*; 2010, **348**, 607-614.

Pagano, C., Boudreaux, B., and Shiomitsu, K. Safety and toxicity of an accelerated coarsely fractionated radiation protocol for treatment of appendicular osteosarcoma in 14 dogs: 10 Gy × 2 fractions. *Vet. Radiol. Ultrasound.*; 2016, **57**, 551-556.

Pasto, A., Bellio, C., Pilotto, G., Ciminale, V., Silic-Benussi, M., Guzzo, G., Rasola, A., Frasson, C., Nardo, G., Zulato, E., Nicoletto, M. O., Manicone, M., Indraccolo, S., and Amadori, A. Cancer stem cells from epithelial ovarian cancer patients privilege oxidative phosphorylation, and resist glucose deprivation. *Oncotarget.*; 2014, **5**, 4305-4319.

Pawlik, T. M. and Keyomarsi, K. Role of cell cycle in mediating sensitivity to radiotherapy. *Int. J. Radiat. Oncol. Biol. Phys.*; 2004, **59**, 928-942.

Quintana, E., Shackleton, M., Sabel, M. S., Fullen, D. R., Johnson, T. M., and Morrison, S. J. Efficient tumour formation by single human melanoma cells. *Nature*; 2008, **456**, 593-598.

Rena, G., Hardie, D. G., and Pearson, E. R. The mechanisms of action of metformin. *Diabetologia*; 2017, **60**, 1577-1585.

Ricci-Vitiani, L., Lombardi, D. G., Pilozzi, E., Biffoni, M., Todaro, M., Peschle, C., and De Maria, R. Identification and expansion of human colon-cancer-initiating cells. *Nature*; 2007, **445**, 111-115.

Rocha, G. Z., Dias, M. M., Ropelle, E. R., Osorio-Costa, F., Rossato, F. A., Vercesi,

A. E., Saad, M. J. A., and Carvalheira, J. B. C. Metformin amplifies chemotherapy-induced AMPK activation and antitumoral growth. *Clin. Cancer Res.*; 2018, **17**, 3993-4005.

Ruoslahti, E. and Reed, J. C. (1994) Anchorage dependence, integrins, and apoptosis. *Cell*; 1994, **77**, 477-478.

Saeki, K., Watanabe, M., Tsuboi, M., Sugano, S., Yoshitake, R., Tanaka, Y., Ong, S. M., Saito, T., Matsumoto, K., Fujita, N., Nishimura, R., Nakagawa, T. Anti-tumour effect of metformin in canine mammary gland tumour cells. *Vet. J.*; 2015, **205**, 297-304.

Samsuri, N. A. B., Leech, M., and Marignol, L. Metformin and improved treatment outcomes in radiation therapy - A review. *Cancer Treat. Rev.*; 2017, **55**, 150-162.

Schipler, A. and Iliakis, G. DNA double-strand-break complexity levels and their possible contributions to the probability for error-prone processing and repair pathway choice. *Nucleic. Acids. Res.*; 2013, **41**, 7589-7605.

Singh, S. K., Hawkins, C., Clarke, I. D., Squire, J. A., Bayani, J., Hide, T., Henkelman, R. M., Cusimano, M. D., and Dirks, P. B. Identification of human brain tumour initiating cells. *Nature*; 2004, **432**, 396-401.

Soeda, A., Inagaki, A., Oka, N., Ikegame, Y., Aoki, H., Yoshimura, S. I., Nakashima, S., Kunisada, T., and Iwama, T. Epidermal growth factor plays a crucial role in mitogenic regulation of human brain tumor stem cells. *J. Biol. Chem.*; 2008, **283**, 10958-10966.

Song, C. W., Lee, H., Dings, R. P. M., Williams, B., Powers, J., Dos Santos, T., Choi, B. H., and Park, H. J. Metformin kills and radiosensitizes cancer cells and preferentially kills cancer stem cells. *Sci. Rep.*; 2012, **2**, 362.

Song, C. W., Park, H., Dusenbery, K., and Cho, C. Metformin potentiates the effects of radiation on cancer stem cells by activating AMPK. *Int. J. Radiat. Oncol. Biol. Phys.*; 2013, **87**, 653-654.

Stahl, J. M., Corso, C. D., Verma, V., Park, H. S., Nath, S. K., Husain, Z. A., Simone, C. B., Kim, A. W., and Decker, R. H. Trends in stereotactic body radiation therapy for stage I small cell lung cancer. *Lung Cancer*; 2017, **103**, 11-16.

Sun, L., Moritake, T., Ito, K., Matsumoto, Y., Yasui, H., Nakagawa, H., Hirayame, A., Inanami, O., and Tsuboi, K. Metabolic analysis of radioresistant medulloblastoma stem-like clones and potential therapeutic targets. *PLoS One*; 2017, **12**, 4.

Takagi, S., Kitamura, T., Hosaka, Y., Ohsaki, T., Bosnakovski, D., Kadosawa, T., Okumura, M., and Fujinaga, T. Molecular cloning of canine membrane-anchored inhibitor of matrix metalloproteinase, RECK. *J. Vet. Med. Sci.*; 2005, **67**, 385-391.

Takahashi, K. and Yamanaka, S. Induction of pluripotent stem cells from mouse embryonic and adult fibroblast cultures by defined factors. *Cell*; 2006, **126**, 663-676.

Tanabe, A., Deguchi, T., Sato, T., Nemoto, Y., Maruo, T., Madarame, H., Shida, T., Naya, Y., Ogihara, K., and Sahara, H. Radioresistance of cancer stem-like cell derived fromcanine tumours. *Vet. Comp. Oncol.*; 2016, **14**, 93-101.

Thamm, K., Graupner, S., Werner, C., Huttner, W. B., and Corbeil, D. Monoclonal antibodies 13A4 and AC133 do not recognize the canine ortholog of mouse and human stem cell antigen prominin-1 (CD133). *PLoS One*; 2016, **11**, 10.

Tirino, V., Desiderio, V., Paino, E., De Rosa, A., Papaccio, F., Fazioli, F., Pirozzi, G., and Papaccio, G. Human primary bone sarcomas contain CD133 (+) cancer stem cells displaying high tumorigenicity *in vivo*. *FASEB J.*; 2011, **25**, 2022-2030.

Vargas, T. H. M., Pulz, L. H., Barra, C. N., Kleeb, S. R., Xavier, J. G., Catao-Dias, J. L., Fukumasu, H., Nishiya, A. T., and Strefezzi, R. F. Immunohistochemical Expression of the pluripotency factor OCT4 in canine mast cell tumours. *J. Comp.*

Pathol.; 2015, **153**, 251-255.

Viale, A., De Franco, F., Orleth, A., Cambiaghi, V., Giuliani, V., Bossi, D., Ronchini, C., Ronzoni, S., Muradore, I., Monestiroli, S., Gobbi, A., Alcalay, M., Minucci, S., and Pelicci, P. G. Cell-cycle restriction limits DNA damage and maintains self-renewal of leukaemia stem cells. *Nature*; 2009, **457**, 51-52.

Visvader, J. E. and Lindeman, G. J. Cancer stem cells in solid tumours: Accumulating evidence and unresolved questions. *Nat. Rev. Cancer.*; 2008, **8**, 755-768.

Wang, M. H., Sun, R., Zhou, X. M., Zhang, M. Z., Lu, J. B., Yang, Y., Zeng, L. S., Yang, X. Z., Shi, L., Xiao, R. W., Wang, H. Y., and Mai, S. J. Epithelial cell adhesion molecule overexpression regulates epithelial-mesenchymal transition, stemness and metastasis of nasopharyngeal carcinoma cells via the PTEN/AKT/mTOR pathway. *Cell Death Dis.*; 2018, **9**, 1.

Wang, W. M., Chen, Y. S., Deng, J. L., Zhou, J. P., Zhou, Y., Wang, S. Y., and Zhou, J. W. The prognostic value of CD133 expression in non-small cell lung cancer: A meta-analysis. *Tumour Biol.*; 2014, **35**, 9769-9775.

Wheaton, W. W., Weinberg, S. E., Hamanaka, R. B., Soberanes, S., Sullivan, L. B.,

Anso, E., Glasauer, A., Dufour, E., Mutlu, G. M., Budigner, G. R. S., and Chandel, N. S. Metformin inhibits mitochondrial complex I of cancer cells to reduce tumorigenesis. *Elife*; 2014, **13**, 3.

Williams, M. V., Denekamp, J., and Fowler, J. F. A review of Alpha-beta ratio for experimental –tumors-implication for clinical-studies of altered fractionation. *Int. J. Radiat. Oncol. Biol. Phys.*; 1985, **11**, 87-96.

Yamamori, T., Yasui, H., Yamazumi, M., Wada, Y., Nakamura, H., and Inanami, O. Ionizing radiation induces mitochondrial reactive oxygen species production accompanied by upregulation of mitochondrial electron transport chain function and mitochondrial content under control of the cell cycle checkpoint. *Free Radic. Biol. Med.*; 2012, **53**, 65-65.

Yamamoto, K., Yasui, H., Bo, T., Yamamori, T., Hiraoka, W., Yamasaki, T., Yamada, K., and Inanami, O. Genotoxic responses of mitochondrial oxygen consumption rate and mitochondrial semiquinone radicals in tumor cells. *Appl. Magn. Reson.*; 2018, **49**, 837-851.

Yamazaki, H., Iwano, T., Otsuka, S., Kagawa, Y., Hoshino, Y., Hosoya, K., Okumura, M., and Takagi, S. SiRNA knockdown of the DEK nuclear protein mRNA enhances apoptosis and chemosensitivity of canine transitional cell carcinoma cells. *Vet.*

J.; 2015, **204**, 60-65.

Yin, S. Y., Li, J. J., Hu, C., Chen, X. Y., Yao, M., Yan, M. X., Jiang, G. P., Ge, C., Xie, H. Y., Wan, D. F., Yang, S. L., Zheng, S. S., and Gu, J. R. CD133 positive hepatocellular carcinoma cells possess high capacity for tumorigenicity. *Int. J. Cancer*; 2007, **120**, 1444-1450.

Zhou, Y. F., Zhou, Y., Shingu, T., Feng, L., Chen, Z., Ogasawara, M., Keating, M. J., Kondo, S., and Huang, P. Metabolic alterations in highly tumorigenic glioblastoma cells Preference for hypoxia and high dependency on glycolysis. *J. Biol. Chem.*; 2011, **286**, 32843-32853.

SUMMARY IN JAPANESE

和文要旨

医療、獣医療において腫瘍に対する放射線治療は重要な役割を果たし、体への負担が少ない有用な治療法である。放射線治療はほとんどの患者において、初期は良好な反応を示し、患者の臨床症状を改善することができる。しかし、いずれは腫瘍の再増大、それに伴う臨床症状の再発を認め、最終的には根治には至らず死に至ることが問題となっている。腫瘍の再増大は、腫瘍細胞内に放射線治療抵抗性の細胞が存在し、放射線治療後に生存、再増殖することが起因となっていると考えられる。そのため、それらの放射線治療抵抗性細胞を同定し、根絶することが新たな放射線治療戦略として望まれている。

Cancer stem-like cells (CSCs) は、放射線治療抵抗性細胞として注目されている。CSCs はがん組織の中で非常に少ない集団であるにも関わらず、DNA 損傷修復能や酸化ストレスを回避する能力が高いことから放射線治療に耐性を示す。そのため、治療によって生き残った CSCs が新たながん細胞を生み出すために、完治することなく再発の起因と成っていると考えられている。しかし、イヌ腫瘍における CSCs の特性、放射線抵抗性および放射線抵抗性機序は不明である。そこで本研究では、イヌ腫瘍の放射線治療抵抗性の原因として CSCs の存在を証明し、それらの特性を解析し、治療の標的とすることで、がんのより高い治療効果や新しい治療の発展に寄与することを最終目的としている。第 1 章では、犬の腫瘍細胞株から、Sphere formation を用いて CSCs を分離し、その性質および放射線反応性の検討を行った。第 2 章では、CSCs に有効な薬剤の探索および放射線抵抗性機序の解明のため、メトホルミンを用いて、その放射線増感効果およびその作用機序についての評価を行った。

第 1 章では、イヌの腫瘍細胞株から CSCs を分離し、放射線反応性を明らかにするため、イヌの骨肉腫、メラノーマ、移行上皮癌および肺腺癌の 4 種細胞株から非足場細胞培養である Sphere formation を用いて分離した球状コロニーの細胞 (Spheroid cells、以下 SCs) について、通常条件の接着培養の細胞 (Adherent cells 、以下 ACs) と比較し、以下の検討を行った。CSCs の形質の解析のために、RT-PCR を用いた CSCs マーカーの発現量の評価、およびマウスへの腫瘍移植試験を用いて腫瘍形成能の評価を実施した。続いて、放射線反応性の解析のため、コロニー形成法を用いて X 線暴露下における生存曲線を作製し、p53-binding protein (53BP1)の集積による X 線暴露後の DNA 損傷の蓄積を評価した。Sphere formation を用いて分離培養した SCs は、ACs と比較して CSCs の形質である *CD133* を始めとした幹細胞マーカーを高発現しており、高い腫瘍形成能を有していた。また、X 線暴露下の各線量において SCs は ACs と比較して高い生存率を示し、SCs は X 線暴露後の DNA の損傷蓄積が少ない結果となった。これらの結果から、Sphere formation を用いて分離した SCs が CSCs の形質および放射線抵抗性を有する CSCs モデルとして適した細胞群であることが示唆され、イヌの腫瘍において、CSCs が放射線感受性を決定する重要な因子であることが示された。

第 2 章では、CSCs を標的とした治療の確立のため、メトホルミンの放射線増感効果およびその作用機序を解析することを目的とした。メトホルミンはミトコンドリアの呼吸鎖を標的として、AMP-activated protein kinase（AMPK）の活性化による mammalian target of rapamycin（mTOR）経路の抑制、およびミトコンドリア呼吸鎖の阻害による活性酸素種（ROS）の増加などの抗腫瘍効果を有するとされてきた。しかし、特に CSCs に対するメトホルミンの放射線増感効果や作用機序は明らかになっていないため、イヌの骨肉腫細胞株から Sphere formation を用いて分離した SCs および対照群として ACs を用い、以下の検討を行った。メトホルミンの放射線増感効果の有無について、コロニー形成法を用いて X 線暴露後の細胞生存率および DNA 損

傷蓄積を評価した。また、メトホルミンのミトコンドリアに対する効果を評価するため酸素消費量、ミトコンドリア膜電位、ATP 産生量および ROS の測定を行った。SCs において、メトホルミンは、放射線照射後の細胞死、および DNA 二本鎖断裂を優位に増加させた。また、放射線増感効果を示した濃度のメトホルミンは、SCs においてミトコンドリアの呼吸活性を優位に抑制し、ミトコンドリア膜電位および ATP 減少させ、細胞内の ROS を増加させることが示された。これらのことから、メトホルミンは SCs に対して、ミトコンドリアの呼吸活性を抑制することで選択的に放射線増感効果を示すことが証明された。さらに、メトホルミンが ACs と比較して SCs に対して放射線増感効果の感受性が高いことについて、ミトコンドリアの呼吸活性について評価を行ったところ、SCs は ACs と比較して呼吸活性が高いことが示された。このことから、ミトコンドリアの呼吸活性は放射線抵抗性に重要な因子となると考えられ、ミトコンドリアを標的としたメトホルミンのような薬剤は CSCs を標的とした治療に有用であることが示唆された。

本研究より、イヌの腫瘍において、CSCs は放射線感受性を決定する因子として重要であることが強く示された。また、CSCs の放射線抵抗性においてミトコンドリアを標的としたメトホルミンが放射線増感薬として有効であることが示され、ミトコンドリアの機能が高いことが CSCs の放射線抵抗性に関与している可能性が示された。